SYNTHESIS OF QUATERNARY AMMONIUM SALTS USING BATCH AND CONTINUOUS TECHNOLOGIES

Marina Ciriani Rodrigues

Thesis to obtain the Master of Science Degree in

Pharmaceutical Engineering

Supervisors: Dr. José Rafael Túlio Antunes

Prof. José Monteiro Cardoso de Menezes

Examination Committee:

Chairperson: Prof. Pedro Paulo de Lacerda e Oliveira Santos

Supervisor: Dr. José Rafael Túlio Antunes

Member of the Committee: Prof. Carlos Alberto Mateus Afonso

July 2017


LISBOA
UNIVERSIDADE
DE LISBOA


Hovione


TÉCNICO
LISBOA


FACULDADE DE
FARMÁCIA
Universidade de Lisboa


iMed.
ULisboa
Research
Institute for
Medicines

“A wise person is made, not born. Wisdom depends on experience, and not just any experience. You need the time to get to know the people you are serving. You need permission to be allowed to improvise, try new things, occasionally to fail and to learn from your failures. And you need to be mentored by wise teachers”

Barry Schwartz

Dedicado aos meus avós.

ACKNOWLEDGEMENTS

Em primeiro lugar, quero agradecer ao Rafael por ter acreditado em mim desde o primeiro dia, por todas as orientações e opiniões que me permitiram evoluir. Pela partilha de entusiasmo e pelo apoio nos momentos menos bons.

Aos professores Carlos Afonso e José Menezes pela ajuda intelectual, motivação, paciência e pela partilha de conhecimentos.

A todos os membros do R&D Produtos, do grupo de produção contínua, alunos de mestrado e doutoramento, entre outros incríveis colegas pela ajuda ao longo do trabalho e pelos momentos de descanso e lazer.

Aos técnicos de laboratório pela ajuda na compra dos materiais e reagentes, pela lavagem dos materiais e pela coordenação do laboratório de forma a que eu pudesse trabalhar sem interrupções e com todos os recursos necessários.

Ao grupo da manutenção, pela rápida disponibilidade a ajudar quando tive dificuldades com os sistemas analíticos.

Aos meus colegas do Grupo de Química Bio-Orgânica do Instituto de Investigação do Medicamento (iMed).

À minha família que apoiou todas as minhas decisões.

Ao Pedro por me incentivar a ser melhor todos os dias, por ser um exemplo de força de vontade e perseverança, por toda a paciência e amor.

Ao quarteto fantástico: Karina, Pedro, Inês e Dinis. Meus melhores amigos.

À Hovione Farmaciência S.A. por ceder as infra-estruturas e pelo apoio financeiro.

RESUMO

Neste trabalho pretendeu-se estudar a síntese de novos sais quaternários de amónio a partir de recursos renováveis. O trabalho abrange (1) a avaliação dos parâmetros reacionais que mais afetam o rendimento em regime descontínuo e contínuo, mudando um parâmetro de cada vez de forma a obter conhecimento da reação e do mecanismo químico. (2) Desenvolvimento do método analítico de cromatografia líquida de alta pressão (HPLC) de forma a monitorizar a reação e desenvolvimento de um método de purificação e isolamento do produto. (3) Desenvolvimento e verificação de um modelo mecanístico (modelo cinético) e de um modelo empírico (desenho de experiências) de forma a prever o rendimento em diferentes condições reacionais, adquirindo um maior conhecimento do processo, determinando os fatores críticos do processo. (4) Determinação de uma zona experimental a partir dos modelos realizados. (5) Verificação da zona experimental e por fim, (6) comparação entre os modelos mecanísticos e empíricos.

Desenvolveu-se um processo para produção de sais quaternários de amónio em regime descontínuo e um processo em regime contínuo. Foi realizada uma abordagem comparativa entre os dois processos.

Os sais produzidos têm aplicação na industria farmacêutica como intermediário para a produção de inibidores da acetilcolinesterase. Neste trabalho, também se propõe um plano de síntese para a produção de uma substância ativa a partir dos sais sintetizados.

Palavras chave: Sais quaternários de amónia; Modelo cinético, Modelo empírico, Síntese Orgânica, Regime Descontínuo, Regime Contínuo.

ABSTRACT

This project is concerned with the synthesis of novel highly functionalised quaternary ammonium salts from renewable resources. Our approach consisted of (1) evaluating the reaction parameters that can affect the production yield changing one factor at a time stablishing a basic understanding of the reaction in batch and in continuous mode. (2) Developing an analytical method for high performance liquid chromatography analysis and defining an appropriate work-up of the crude. (3) Developing and evaluating a mechanistic (kinetics) and an empirical (design of experiments) model to predict the formation of the product and the most relevant reaction constituents in terms of process performance, this way stablishing a deeper understanding of the reaction in batch and in continuous mode. (4) Defining a design space based on the model output, (5) verifying the design space through experimental testing and (6) comparing the two types of model (mechanistical and empirical) that was made.

A process was developed for this new plan of synthesis in batch, and a process in continuous, defining and appropriate set-up of the system and comparing the advantages and disadvantages of both.

The quaternary ammonium salts synthesized has application in pharmaceutical industrial as an intermediate to produce acetilcolinesterase inhibitors and with this work it is proposed a plan of synthesis to produce an active pharmaceutical ingredient from those salts.

Keywords: Quaternary ammonium salts; Mechanistic Modelling, Empirical Modelling, Organic Synthesis, Batch Manufacturing, Continuous Manufacturing, Design Space.

TABLE OF CONTENTS

LIST OF FIGURES

LIST OF TABLES

LIST OF ABBREVIATIONS

ACh - Acetylcholine

AChE - Acetylcholinesterase

API – Active Pharmaceutical Ingredient

CM – Continuous Manufacturing

Cp – Heat Capacity

CPP – Critical Process Parameter

CQAs – Control Quality Attributes

DFT – Density Functional Theory

DoE – Design of Experiments

Ea – Activation Energy

FEP - Fluorinated Ethylene Propylene

HPLC – High Performance Liquid Chromatography

ICH - International Conference on Harmonisation

K_c – Kinetic Constant

LLE – Liquid-Liquid Extraction

NDA – New Drug Application

NMR – Nuclear Magnetic Resonance

NRTL - Non-random two-liquid

PAT – Process Analytical Technology

PCA – Principal Component Analysis

PFA - Perfluoroalkoxy Alkanes

PLS – Partial Least Square

PTFE - Polytetrafluoroethylene

QbD – Quality by Design

$Rt_{ref.}$ – Residence time of reference

SST – Stainless Steel

$T_{ref.}$ – Temperature of reference

$Time_{ref.}$- Time of reference

US-FDA – United States, Food and Drugs Administration

1. GENERAL INTRODUCTION

Manufacturing of drug products is controlled by a regulatory framework that safeguards the quality of the final product providing quality pharmaceuticals to the public. Over the last years, there has been growing interest in increasing the safety and quality of medications while simultaneously cutting the cost of manufacturing by implementing more structured process development. With the encouragement of US Food and Drugs Administration (FDA), today the pharma explores opportunities for improving pharmaceutical development, manufacturing, and quality assurance through innovation in product and process development, process analysis, and process control.[1]

Currently, pharmaceutical manufacturing is developing through enhanced and enabling technologies complementing the traditional batch based processes with continuous manufacturing to explore new chemistry, improve safety, reduce industrial footprint and investment.[2]

Implementation of process analytical technology (PAT) and digital data processing allow for close loop quality control systems and real-time release. The goal of PAT is to enhance understanding and control the manufacturing process, which is consistent with the current drug quality system: quality cannot be tested into products; it should be built-in or should be by design.[1,3] An example of it are novel manufacturing methods (e.g., based on continuous flow chemistry) that are now being introduced by industry, academia, and regulators.[4–6] Moreover, the International Conference on Harmonisation of Technical Requirements for Registration of Pharmaceuticals for Human Use (ICH) is developing a new guideline ICH Q12 that will provide a framework to facilitate the management of post-approval chemistry, manufacturing and controls changes in a more, transparent and efficient manner across the product lifecycle. This way, encouraging companies to develop and register more enhanced Quality by Design (QbD) approaches and providing tools to introduce more innovative approaches to manufacturing across the ICH regions.[7,2]

In recent years, pharmaceutical industry, regulatory agencies, and academia have become interested in the development of technologies for the continuous manufacturing of drug products. Many examples have been published referring improvements in process efficiency or controllability by using CM, driving applications have involved the invention of very fast or high-pressure organic chemistry pathways that can only be operated and studied in small-scale continuous-flow reactors.[8,9]

A typical process for manufacturing an active pharmaceutical ingredient (API) is influenced by many parameters, including critical process parameters (CPPs) and critical quality attributes (CQAs). Those parameters can interact to each other and these interactions could be difficult to understand and have effects on the quality of the product.[10] Consequently, statistical

design of experiments (DoE) methods are extensively applied in process design to help scientists understand the effects of possible multidimensional combinations and interactions of various parameters on product quality. Application of a DoE strategy provides scientific understanding of the process parameters and leads to establishment of a design space and manufacturing control strategy. Therefore, building high quality and validated models of process systems is key to many applications such as model based product and process design, control and optimization. DoE is an important tool between the experimental and modelling world called as "model-based experiment design".[11]

The unmistakable trend away from the traditional quality by testing and toward QbD has led to increased awareness of the concept of design space.[12] DoE plays a central role defining the acceptable ranges for the critical process parameters. The FDA now expects DoE to be part of the NDA submissions.[13,14]

Furthermore, several of the well-known green chemistry principles advocate for using lesser amounts of solvents and reagents and for increased process efficiency as a means toward generating less chemical waste. Accordingly, manufacturers are increasingly implementing programs to assess the green chemistry performance of their processes. DoE's ability to enable scientists to hone in on the optimal reaction conditions has helped it gain wider acceptance. Clearly the perceived barriers[15] to implementing DoE in the process chemistry setting are being overcome, leading to wider adoption of this tool.

CHOLINESTERASE INHIBITORS

Reversible cholinesterase inhibitors form a transition state complex with the enzyme acetylcholinesterase (AChE) just as acetylcholine (Figure 1) does.[16] These compounds contain a carbamate group that forms a reversible covalent bond with acetylcholinesterase and compete with acetylcholine in binding the active sites of the enzyme.[16] The chemical structure of classic reversible inhibitors such as API-X and others shows their similarity to acetylcholine. These compounds have a high affinity with the enzyme and their inhibitory action is reversible. These inhibitors differ from acetylcholine in that they are not easily broken down by enzymes. Enzymes are reactivated much slower that it takes for subsequent hydrolysis of acetylcholine to happen. Therefore, the pharmacological effect caused by these compounds are reversible.[17]

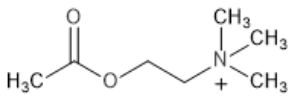

Figure 1 - Chemical Structure of Acetylcholine

1.1. QUATERNARY AMMONIUM SALTS

Quaternary ammonium salts are unsaturated heterocyclic compounds. The usual precursor is pyridine, which is derived either from coal tar or may be synthetically prepared.[18] These salts are generally known as cationic surfactants, have bacteriostatic properties and can be used as sanitizing or antiseptic agents, as components in cosmetic formulations, as germicides and fungicides. Additionally, they are used as antistatic agents, corrosion inhibitors and textile softeners.

Quaternary ammonium salts are employed in pharmaceuticals such as acetylcholinesterase inhibitors[19], for gene delivery and exhibit anti-inflammatory activity.[20] Cytotoxic agents such as 12-methacryloyloxydodecylpyridinium (mdpb) and cetylpyridinium chloride (cpc), are used extensively for the treatment of oral infections.[21]

Moreover, those salts have high synthetic value as key intermediate to produce wide range of pharmacologically relevant piperidine, dihydro, tetrahydropyridine frameworks. An intensive research have also been carried out with the use of quaternary ammonium salts as a key substrate for the synthesis of various natural product cores. Compounds such as 4-amino-1-alkyl pyridinium s are shown to exhibit interesting antimicrobial activity and biological activities such as anti-bacterial activity against *Escherichia coli* and *Staphylococcus aureus*.[22]

QUATERNARY AMMONIUM SALTS AS IONIC LIQUIDS

Ionic liquids are salts, completely composed of ions, and generally are liquid below ($T_{ref.}$ + 30)ºC.[24] They present some interesting physical and chemical properties, for example small vapour pressure, non-flammability, and high solvation potential that permit them to be classified as green solvents.[25] Those physical and chemical properties could be change by varying both the cation and the anion which give them a notable advantage. Their properties are enabling rapid advances in numerous applications, including processes at an industrial scale: BASF (aluminium plating, cellulose dissolution), Institut Français du Pétrole (difasol), Degussa (paint additives), Linde (hydraulic ionic liquid compressor), Pionics (batteries), and G24i (solar cells).[26]

Ionic liquids are also providing unexpected opportunities at the interface of chemistry with the life sciences acting as solvents in enzymatic and whole-cell bio catalysis and as protein stabilisation agents. In addition, their potential use as active pharmaceutical ingredients, though still rather exploratory, further highlights their potential in biochemical studies. Indeed, ionic liquids have featured extensively in recent scientific literature and patents, which reflects their importance in research and development.

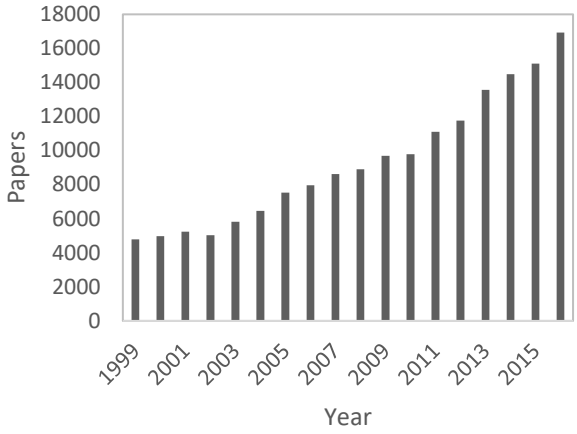

Figure 2 - Number of papers on the use of ionic liquids published per year (via Science Direct)

2. OBJECTIVES

This thesis is about the synthesis of novel functionalised quaternary ammonium salts, namely *product P*, from reagent A with the objective to further produce API-X . There are many advantages in using the proposal synthesis:

1. Reagent A can be easily synthesised and is commercially available;
2. The reagents are low cost;
3. Can be used in a one-step synthesis;
4. Bio-renewable resources (sustainability)

Our objectives were:

To develop a process to produce quaternary ammonium salts in batch:

(1) Identify the reaction parameters that can affect the production yield changing one factor at a time stablishing a basic understanding of the reaction using batch technologies. In parallel of that, developing an analytical method to monitor the reactions and define an appropriate work-up and isolation procedure of *product P* (2) develop and evaluate a mechanistic and an empirical model for the synthesis of *product P*, and the most relevant process parameters (catalyst, temperature, pressure etc), this way stablishing a deeper process understanding (3) define a design space based on the model output and (4) verify the design space through experimental testing.

Develop a process to produce quaternary ammonium salts using flow conditions:

(1) Define the set-up to use (using microchannels, coils in vertical or horizontal, etc) (2) developing and evaluating mechanistic and empirical model for the synthesis of *product P*, and the most relevant process parameters (residence time, equivalents of catalyst, etc) (3) Define an online control system using PAT; (4) define a design space based on the model output and (5) verify the design space through experimental testing. These aspects may be relevant and applicable to future filings in a QbD approach.

To produce API-X :

Develop an industrially scalable process to produce API-X from *product P*.

3. SYNTHESIS OF QUATERNARY AMMONIUM SALTS USING BATCH TECHNOLOGIES

3.1. RESULTS AND DISCUSSION

The objective of this thesis was to obtain *product P* which consists in a quaternary ammonium salt from reagent A and B, determining the best conditions to synthesize it.

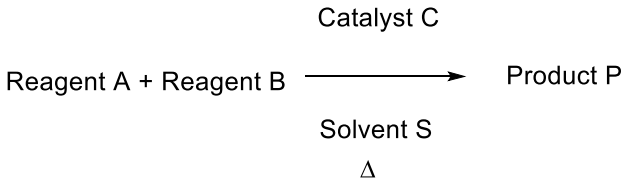

3.2.1. BATCH REACTIONS WITH REAGENT B

The batch tests were performed at a 10 mg scale. The reaction was carried out in a high-pressure vessel since the boiling point of solvent S is low. The work up was performed using activated charcoal.[27] We performed ^{1}H-NMR analysis after the reaction completion.

EFFECT OF CATALYST

The reactions were performed by using bronsted and lewis acids as catalysts.

Table 1 - First reactions to produce product P using: 100mM, a value between [0-2] equivalents of catalyst, a value between [1-4] equivalents of reagent B, during ($time_{ref.}$ + 9) h at $T_{ref.}$

Reference	Catalyst	Observation of *product P*
MCR01	Catalyst A	[0-20]%
MCR02	Catalyst C	[0-20]%
MCR03	Catalyst B	[0-20]%

Table 2 - First reactions to produce product P: $T_{ref.}$ºC, 100mM, a value between [0-2] equivalents of catalyst, a value between [1-4] equivalents of reagent B, during ($Time_{ref.}$ + 11) h

Reference	Catalyst	Observation of *product P*
MCR04	Catalyst D	[0-20]%
MCR05	Catalyst F	[0-20]%

MCR06	Catalyst G	[0-20]%
MCR07	Catalyst H	[0-20]%
MCR08	Catalyst I	[0-20]%
MCR09	Catalyst J	[0-20]%

By doing those reactions, we notice that in three hours, the reactions changed of colour from yellow to black.

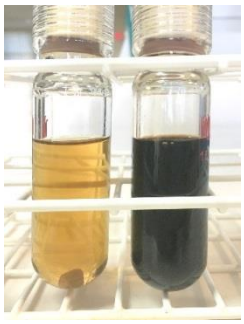

Figure 3 - Time zero of a reaction (MCR02), where reagent A gives the yellow color (left) and time seventeen of the same reaction (right)

It was visualized formation of by-products during time that attached to the glass of the high-pressure vessel that can be seen in Figure 4.

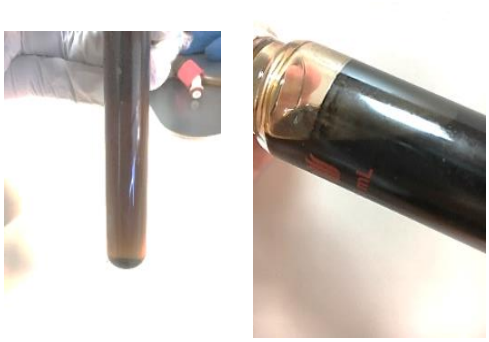

Figure 4 - Observation of by-products formation. On the left it is observed sedimented solids in the bottom of the tube. On the right it is observed precipitated at the walls of the high pressure vessel

The reaction with catalyst C (MCR02) was cleaner than the other ones. The reaction with catalyst B (MCR03) was the one that presented a smaller integration of the shifts in the H-NMR using D_2O as solvent.

Later, with the HPLC method developed, we obtained the UV-Vis spectra of the components of the reactional mixture. [28]

Color changes due to an increasing number of conjugated double bonds thereby increasing the wavelength of light absorption. We can observe this on the spectra where the by-product presents a maximum absorbance at X nm against reagent A, X-25 nm.

Moreover, it was performed mass spectroscopy to determine the mass of the by-product.

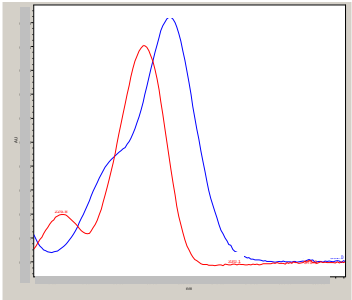

Figure 5 - UV-Vis spectra of Reagent A (red) and side product (blue)

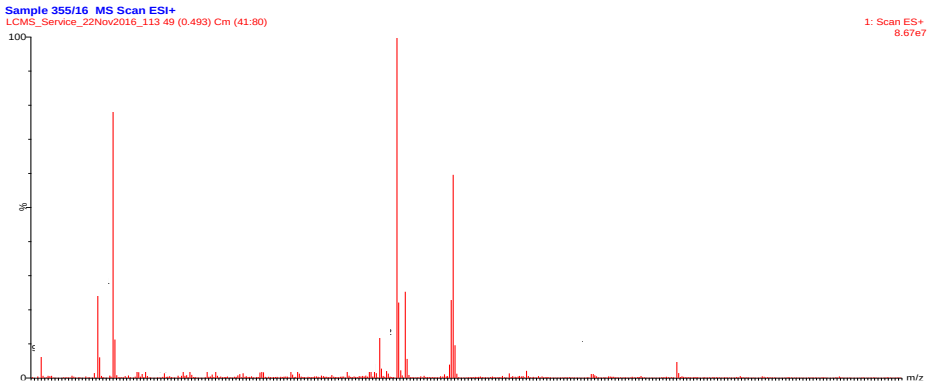

Figure 6 - Mass Spectra of MCR02

To continue the one factor at a time approach, it was performed reactions with different times and temperatures at the same concentration with catalyst C and catalyst A to study the influence of these two parameters.

EFFECT OF TEMPERATURE AND TIME

Table 3 - Effect of temperature and time using a value between [0-2] equivalents of catalyst C, [1-6] equivalents of reagent B and solvent S, 100mM

Catalyst A			
Reference	Time (h)	Temperature (ºC)	Yield
MCR10	$Time_{ref.}$-10	$T_{ref.}$-50	[0-20]%
MCR11	$Time_{ref.}$-10	$T_{ref.}$-30	[0-20]%
MCR12	$Time_{ref.}$.-10	$T_{ref.}$-10	[0-20]%
MCR13	$Time_{ref.}$-10	$T_{ref.}$	[0-20]%
MCR14	$Time_{ref.}$+11	$T_{ref.}$	[0-20]%
MCR15	$Time_{ref.}$+33	$T_{ref.}$	[0-20]%
MCR16	$Time_{ref.}$+57	$T_{ref.}$	[0-20]%

Table 4 - Effect of temperature and time using a value between [0-2] equivalents of catalyst C, [1-6] equivalents of reagent B and solvent S, 100mM

Catalyst C			
Reference	Time (h)	Temperature (ºC)	Yield
MCR17	$Time_{ref.}$-10	$T_{ref.}$-50	[0-20]%
MCR18	$Time_{ref.}$-10	$T_{ref.}$-30	[0-20]%
MCR19	$Time_{ref.}$-10	$T_{ref.}$-10	[0-20]%
MCR20	$Time_{ref.}$-10	$T_{ref.}$	[0-20]%
MCR21	$Time_{ref.}$+9	$T_{ref.}$-50	[0-20]%
MCR22	$Time_{ref.}$+9	$T_{ref.}$	[0-20]%
MCR23	$Time_{ref.}$+33	$T_{ref.}$-50	[0-20]%
MCR24	$Time_{ref.}$+33	$T_{ref.}$	[0-20]%
MCR25	$Time_{ref.}$+57	$T_{ref.}$-50	[0-20]%
MCR26	$Time_{ref.}$+57	$T_{ref.}$	[0-20]%

In fact, with those reactions it is observed that temperature have impact in the process since the yield, even low, improves with higher temperatures. The impact in the process of the time of reaction and the catalyst (catalyst A or catalyst C) are still not clear/conclusive but the ones that are lewis acids presented better yields. To continue this approach, the reactions were performed using catalyst C as catalyst to understand the impact of another parameters in the process. In the subsection 4.2.6 a study of three different catalysts was carried out using statistical design of experiments.

EFFECT OF THE NUMBER OF EQUIVALENTS OF CATALYST AND TIME

We performed reactions changing the equivalents of catalyst C (the reactions mentioned above were performed using a value between [0-2] equivalents of the lewis acid) in a way to understand the effect of the presence of it in the reaction.

Table 5 - Effect of the number of equivalents of catalyst and time in the process using [1-6] equivalents of reagent B and solvent S, 100mM

Catalyst C

Reference	Nº Equivalents of catalyst	Time (h)	Temperature (ºC)	Yield (%)
MCR27	[0-2]	$time_{ref.}$ + 9	$T_{ref.}$	[0-20]
MCR28	[0-2]	$time_{ref.}$ + 33	$T_{ref.}$	[0-20]
MCR29	[0-2]	$time_{ref.}$ + 57	$T_{ref.}$	[0-20]
MCR30	[0-4]	$time_{ref.}$ + 9	$T_{ref.}$	[0-20]
MCR31	[0-4]	$time_{ref.}$ + 33	$T_{ref.}$	[0-20]
MCR32	[0-4]	$time_{ref.}$ + 57	$T_{ref.}$	[0-20]

This study was not conclusive since the results were not consistent. MCR29 presented a yield of 0% while MCR28 and MCR29 presented a yield between [0-20]%, which corresponds the same yields of using less equivalents of catalyst.

EFFECT OF THE NUMBER OF EQUIVALENTS OF REAGENT B

To study the effect of the equivalents of reagent B in the process, we carried on reactions with values between [1-6] equivalents of this reagent, changing time, equivalents of catalyst (catalyst C) and temperature.

Table 6 - Effect of the number of equivalents of catalyst C, temperature and time when using a value between [1-6] equivalents of reagent B, 100mM.

Catalyst C				
Reference	Nº equivalents of catalyst	Time (h)	Temp. (ºC)	Yield (%)
MCR33	[0-2]	$time_{ref.}$ + 9	$T_{ref.}$	[0-20]
MCR34	[0-2]	$time_{ref.}$ + 33	$T_{ref.}$	[0-20]
MCR35	[0-4]	$time_{ref.}$ + 9	$T_{ref.}$	[0-20]
MCR36	[0-4]	$time_{ref.}$ + 33	$T_{ref.}$	[0-20]
MCR37	[0-4]	$time_{ref.}$ + 9	($T_{ref.}$ + 30)ºC	[20-40]
MCR38	[0-4]	$time_{ref.}$ + 33	($T_{ref.}$ + 30)ºC	[20-40]

The effect of time in the process still not conclusive but with these 39 reactions we can conclude that $time_{ref.}$ + 9 hours is enough. A deeper study of the time for reaction completion was carried out in the subsection 4.2.5. when it was made a kinetic study.

Temperature is an important parameter, it was reached yields between [20-40]% increasing 30ºC of the reference temperature ($T_{ref.}$). The use of a higher number of equivalents of reagent B improved the yields.

Some results were not consistent (MCR35), at this stage it was considered to change the work-up strategy, avoiding the use of activated charcoal. (The work up strategy is found in the subsection 4.2.2.).

EFFECT OF SOLVENT

We studied different solvents with different properties than solvent S but no solvent presented increasing in the yield.

Table 7 - Solvents used in the conditions

Reference	Solvent	Yield (%)
MCR40	Solvent R	[0-20]
MCR41	Solvent U	[0-20]
MCR42	Solvent V	[0-20]
MCR43	Solvent X	[0-20]

CONCLUSION

With this approach changing one factor at a time we concluded that 24 hours is enough, (ii) we tried, in the same conditions, to do the reactions in a high pressure reactor and in a round bottom flask to compare the effect of pressure in the system and we conclude that pressure is needed, (iii) we observed formation of by-products even if solution is more diluted, (iv) we observed that temperature is a critical parameter, (v) the best catalyst until now is catalyst C, (vi) the best solvent until now is solvent S.

3.2.2. DEVELOPMENT OF WORK-UP

The initial work up used was:

1. Diluting the reactional mixture in water (50mL) and mixing it with activated charcoal.
2. Filtration of the activated charcoal and evaporation of the solvent at low pressure.

This work up purified the reaction mixture but we still have excess of reagent B in the solution.

To eliminate the excess of the reagent B, we developed an improved work-up using liquid-liquid extraction (LLE).

1. We diluted the reactional mixture with water (50mL) and adjusted to pH [11-15] with a solution of NaOH 1M (Since pKa of reagent B is high between [9-11]). This way we guarantee that all reagent B is neutralized;
2. Perform a liquid-liquid extraction, washing the reactional mixture with an appropriate solvent (3x50mL) at room temperature;
3. Added activated charcoal in the aqueous phase, mixing the suspension and then filtrating solids with a filter G4;
4. Evaporate the solvent at reduced pressure.

After developing the HPLC method (subsection 4.2.3.), it was verified that the use of activated charcoal causes significant product loss. (We inject on HPLC three samples: a sample without work-up, after LLE and after the filtration of activated charcoal). The peak area of *product P* decreased considerably after the third step – filtration of activated charcoal. Additionally, we verified that the LLE removes not only the excess of reagent B, but also impurities in the reactional mixture.

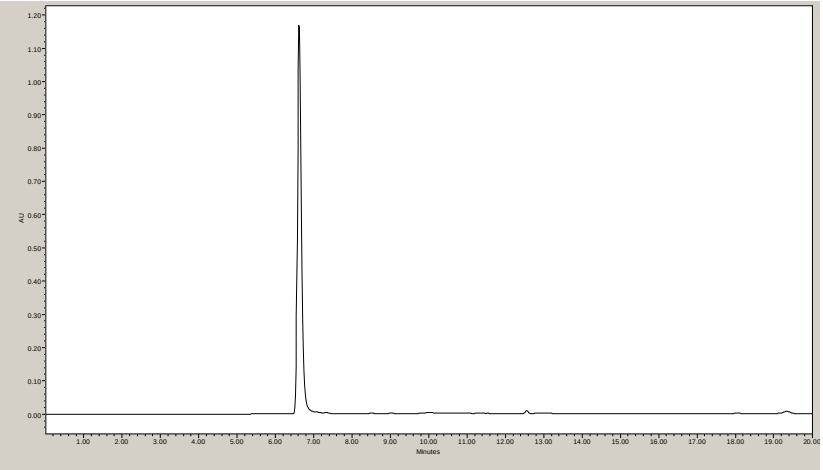

Figure 7 - Chromatogram of a sample after LLE with an appropriate solvent

3.2.3. HPLC METHOD DEVELOPMENT

According to Pharmacopeia 8.0, the chromatographic procedure for API-X may be carried out using a stainless-steel column 0.25 m long and 4.0 mm in internal diameter packed with base-deactivated octadecylsilyl silica gel for chromatography;

Since the main goal of the work is to synthesize API-X, for the first step of the process (reagent A to *product P*) we decided to try to use the same type of column.

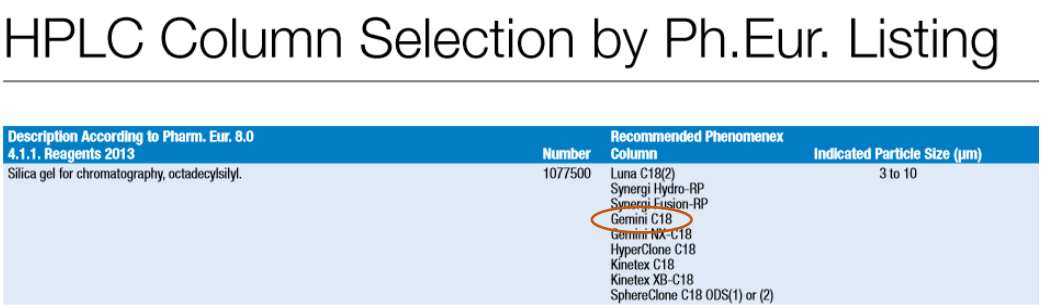
HPLC Column Selection by Ph.Eur. Listing

Description According to Pharm. Eur. 8.0 4.1.1. Reagents 2013	Number	Recommended Phenomenex Column	Indicated Particle Size (µm)
Silica gel for chromatography, octadecylsilyl.	1077500	Luna C18(2) Synergi Hydro-RP Synergi Fusion-RP Gemini C18 Gemini NX-C18 HyperClone C18 Kinetex C18 Kinetex XB-C18 SphereClone C18 ODS(1) or (2)	3 to 10

Figure 8 - Types of Phenomenex® Columns base-deactivated octadecylsilyl silica gel for chromatographic systems. (Reproduced from)

In the first three tests, we used a Gemini C18 *Phenomenex*® reversed phase column with 5 µm of internal diameter, 0.25m long. UV Detection: 250 nm

Test 1:

Mobile phase A was 0.1% (v/v) trifluoroacetic acid (TFA) in water; mobile phase B was 0.1% (v/v) TFA in acetonitrile. The flow rate was maintained at 1.0 mL/min for ($Rt_{ref.}$ + 10) min, starting with a ratio of 95% A and 5% B to 5% A and 95% B; Temperature: 25ºC; 20 µL sample injection.

There was no selectivity in the peaks.

Test 2:

Mobile phase A was water; mobile phase B was acetonitrile. The flow rate was maintained at 1.0 mL/min for 15 min in an isocratic mode with a ratio of between 90% A and 10% B. Temperature: 25ºC. 20 µL sample injection.

There was no selectivity in the peaks.

Test 3:

Mobile phase A was water; mobile phase B was acetonitrile. The flow rate was maintained at 1.0 mL/min for 20 min, phase gradient starting with a ratio of 95% A and 5% B to 5% A and 95% B. Temperature: 25ºC. 20 µL sample injection.

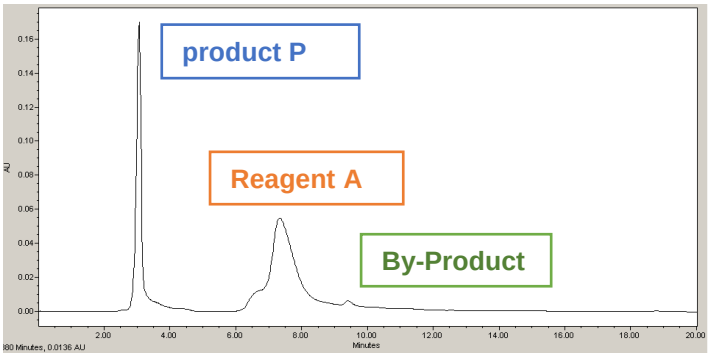

Figure 9 - Chromatogram with Gemini-C18 5µm internal diameter, 250 nm

Since the peal of reagent A was not so sharp, we performed a overmore test using a Gemini C18 *Phenomenex*® reversed phase column with 3 µm of internal diameter, 0.25m long:

Test 4

Phase A was water; phase B was acetonitrile. The flow rate was maintained at 1.0 mL/min for 20 min, starting with a ratio of 95% A and 5% B to 5% A and 95% B. Temperature: 25ºC. 20 µL sample injection.

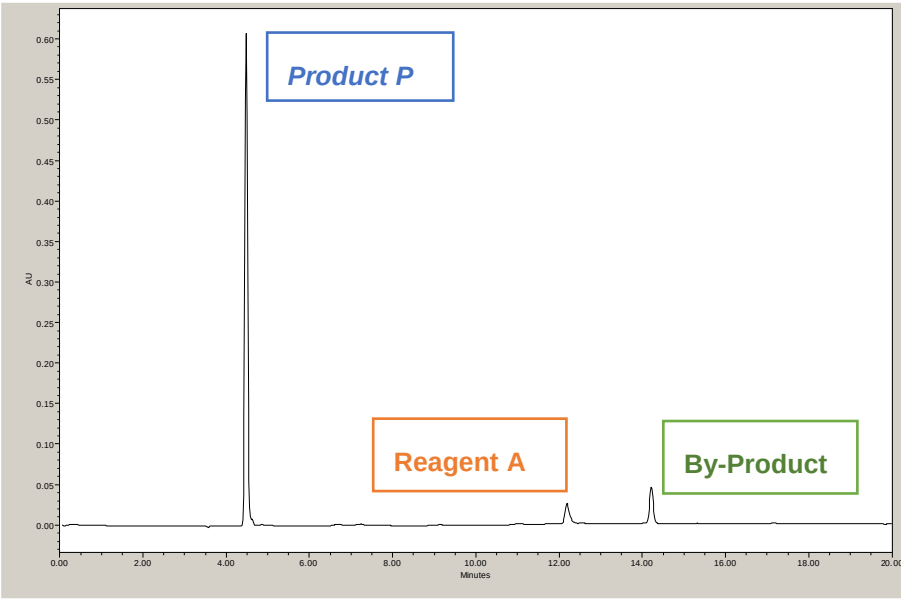

Figure 10 - Chromatogram with Gemini C18 3µm internal diameter, 250 nm

- The column was conditioned in 30% water and 70% acetonitrile.
- The equilibration time was 30 minutes before the first injection of the day and 10 minutes between injections.

The UV detection wavelength was chosen considering the maximum absorbances of reagent A and *product P*.

Table 8- Retention times of the components

Components	Retention Time (min)
Product P	6.60
Reagent A	14.92
By-product	17.73

With an HPLC method defined, we could perform the calibration curves for Reagent A and *product P*:

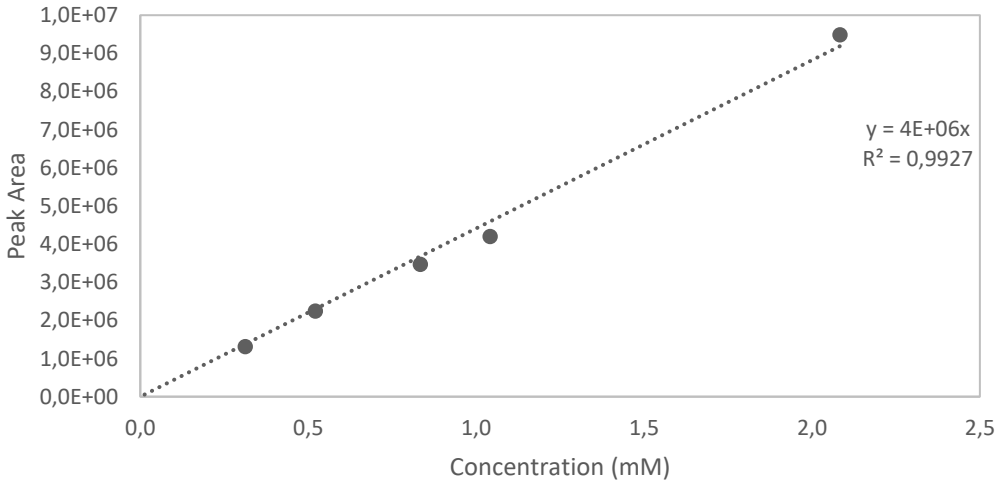

Figure 11 - Calibration curve of Reagent A

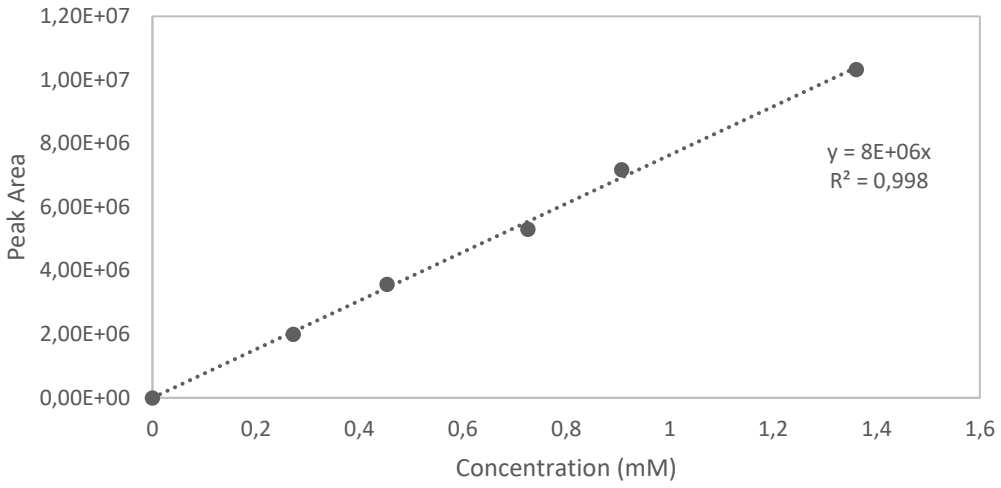

Figure 12 - Calibration curve of product P

Concluding, we developed a gradient method to analyse the reaction of synthesis of *product P* from reagent A that is very reproducible (analysis was performed in different HPLC systems during the work).

3.2.4. MECHANISTIC MODELLING (KINETIC STUDY)

To study the synthesis of product P over time (kinetic study) in batch and to further construct a model of the reaction on dynochem®, we used two different temperatures - $T_{ref.}$ and ($T_{ref.}$ + 30)ºC to perform the reaction.

We followed the formation of product by HPLC analysis using the method mentioned previously. We collected samples hourly, during [$time_{ref.}$ + 1] hours, and injected the solution in the HPLC (1 mM). In the first hours of the reaction, we could observe that the peak area of *product P* was growing linearly and in the lasts hours the area maintained constant. At $T_{ref.}$ it took [$time_{ref.}$ – 3] hours to obtain the maximum area of the peak of product, obtaining yields between [0-20]% while at ($T_{ref.}$ + 30)ºC it took [$time_{ref.}$ – 6] hours (Figure 13) obtaining yields between [20-40]%. With this study we can conclude that the temperature is a critical parameter that affects not only the velocity of the reaction but the yield as well, with highest temperatures, the main reaction is faster and presents better yields.

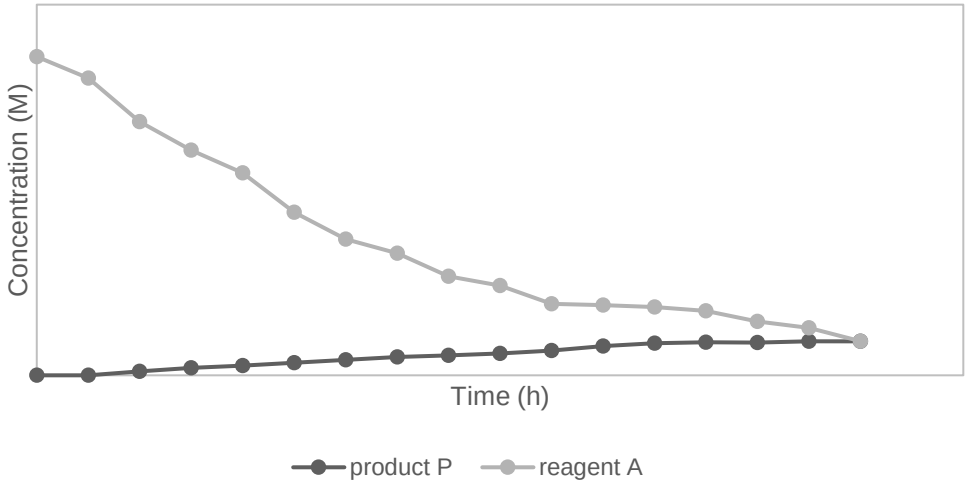

Figure 13 - Kinetic Study in Batch at $T_{ref.}$. In a high pressure vessel it was added reagent A, 15 mL solvent S, a value between [1-6] equivalents of reagent B and a value between [0-4] equivalents of catalyst C.

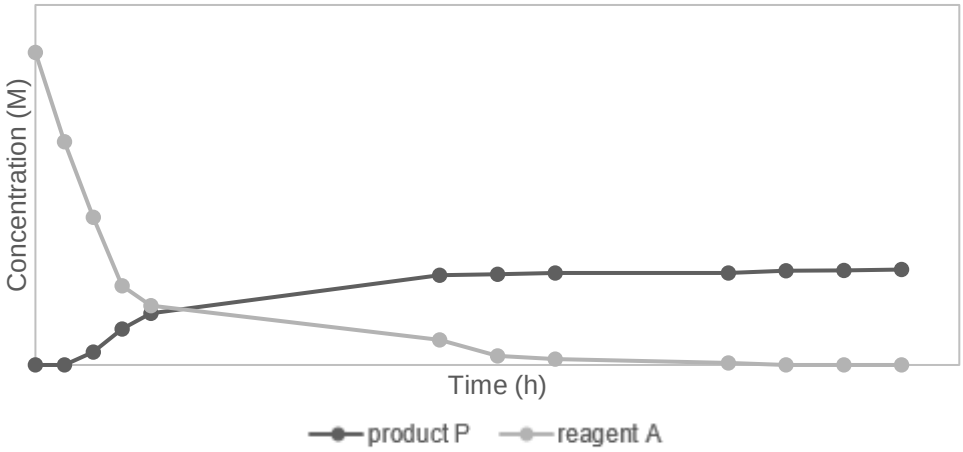

Figure 14 - Kinetic Study in Batch at ($T_{ref.}$ + 30)ºC. In a high pressure vessel it was added reagent A, 15 mL of solvent S, a value between [1-6] equivalents of reagent B and a value between [0-4] equivalents of catalyst C.

To construct the model on Dynochem® we must add all the information about components and its molecular weight, concentrations, reactional mechanism, all the conditions that the reactions were performed and the mass balance must be correct.

Because we have a reagent that is in gas phase in the temperature used (reagent B), gas solubility will play a role because gas-liquid reactions occur in solution with soluble gas. Henry's law is used to quantify the solubility of gases in solvents where the partial pressure (p) is related to the concentration of gas in solution (c) by a temperature-dependent constant (k_H).

$$p\,(reagent\ B) = K_H \times c(reagent\ B) \quad \textbf{(1)}$$

And total mass transfer between gas and liquid phase is expressed:

$$\frac{d[reagent\ B]}{dt} = K_{LA}[c^*(reagent\ B) - c(reagent\ B)] \quad \textbf{(2)}$$

K_{LA} – Mass coefficient between liquid and gas phase.

C*(reagent B) – is the value of concentration of reagent B in the gas phase.

C(reagent B) - is the value of concentration of reagent B in the liquid phase.

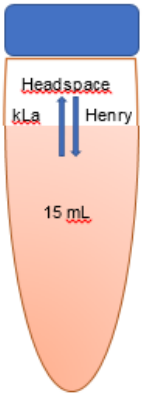

Figure 15. Mass transfer of reagent B between liquid and gas phase

To simplify the model, and since we used a high pressure vessel, we considered that all reagent B is in liquid state inputting that in the model, so as it can be seen in Figure 16, there is approximetly 0 M of reagent B in gas phase.

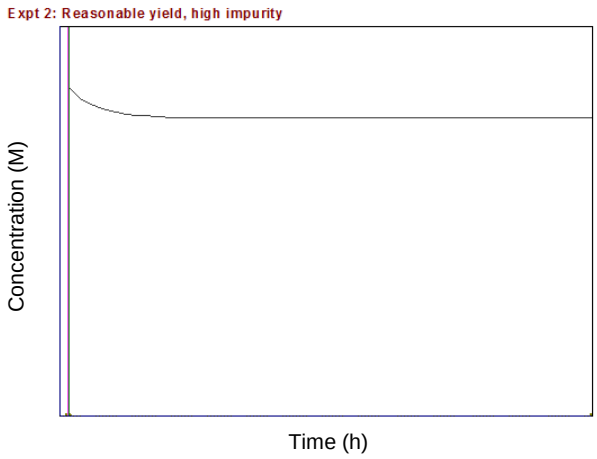

Figure 16 - Concentration of Reagent B in gas phase during the reaction (Model)

As illustrated in Figure 17, the reaction pathway involves (1) reagent A combines with the catalyst to form intermediate I, this way activating the C–O bond of reagent A (2) a nucleophilic attack of reagent B to intermediate I forming the product P.

No other side reactions were found to occur to a significant extent to influence the reactions of interest.

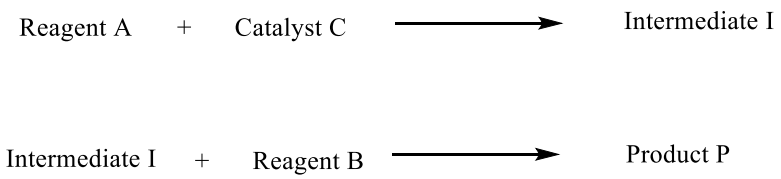

Figure 17 - Reaction scheme for (1) reagent A combines with the catalyst to form intermediate I, this way activating the C–O bond of reagent A (2) a nucleophilic addition of reagent B to intermediate I forming the product P.

DynoChem® modelling software was employed to regress the Arrhenius parameters and simulate different model scenarios (Annex D). The experimental data for model parameter regression was obtained by conducting 10mg scale experiments that varied the reaction temperature from $T_{ref.}$ to ($T_{ref.}$ + 30)ºC. Based on prior knowledge and experience, these parameters ranges were sufficiently broad to encompass the likely design ranges and to explore potential edges of failure. A set of parameters were estimated K_{c1}, K_{c2}, K_{c3}, K_{c4}, E_a for each batch reaction (Table 10) by fitting the proposed model with the concentration profiles obtained using an HPLC system, minimizing the error of each parameter.

For each experiment, ten samples were analyzed by HPLC (in different time of reaction) to measure the content of starting material and product. With this, we obtained a model that fits with the experimental data and this way, we could determine the activation energy (E_a) and the kinetic constant (K) of the reaction in batch, obtaining the parameters of Ahrrenius equation.

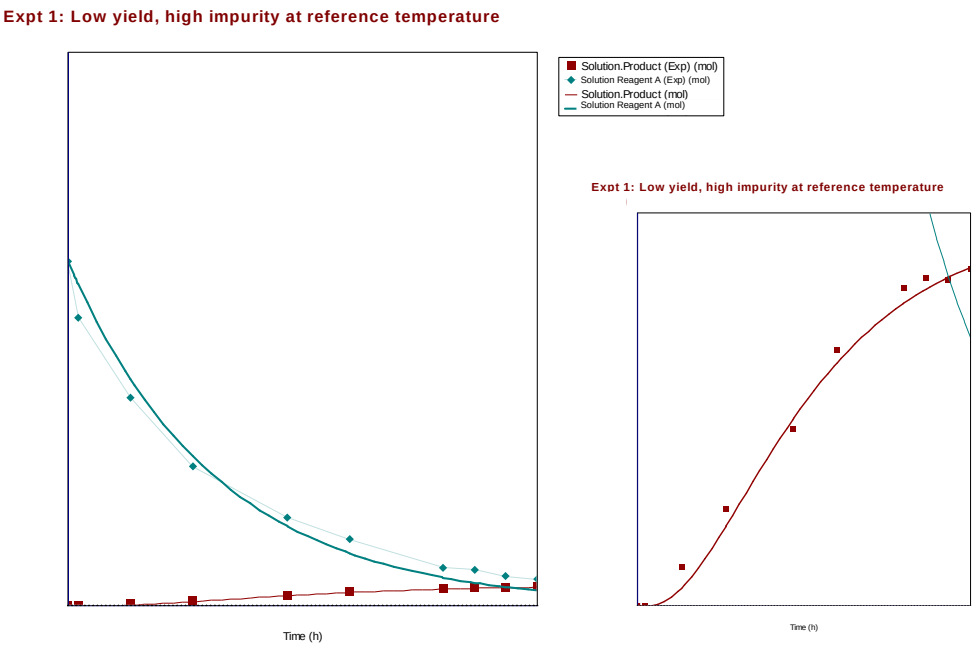

Figure 18 - Model of Dynochem® for batch reaction. Solid lines represent the model prediction, and circles represent the experimental values.

The least squares optimality criterion minimizes the sum of squares of residuals between actual observed outputs and outputs values of the numerical model that are predicted from input observations. In this case, Dynochem® gives us the sum of squares quadratic (SSQ) and this value can be interpreted as the sum of the errors between the predicted values and the observed ones of all points (in this case, we have 10). The lower is SSQ, the better is the fitting of the model.

Table 9 - Sum of squares quadratic, expt 1: Low yield, high impurity at reference temperature

Data profile name	Number of Points	SSQ	Coef. of Determination
Solution.Reagent A	10.0	**0.0186**	0.9817
Solution.Product	10.0	**0.0281**	0.9826

With the model fitted, we could determinate the kinetic parameters of the chemical mechanism:

Table 10 - Parameters for batch reactions after fitting the model. (Kinetic constant and Activation Energy)

Reaction	Ea (kJ/mol)	K	Confidence interval
1	[30-200]	[1.00E-4 to 9.00E-2] L/mol.s	22.3%

2	[100-300]	[1.00E-6 to 9.00E-2] L/mol.s	14.1%

Table 11 - Rate Expressions for each reaction studied: (1) reagent A combines with the catalyst to form intermediate I, this way activating the C–O bond of reagent A (2) a nucleophilic addition of reagent B to intermediate I forming the product P.

Reaction	Rate Expression
1	$\frac{\mathrm{d}[\text{Intermediate I}]}{\mathrm{dt}} = \mathrm{K}_1 \times [\text{Reagent A}] \times [\text{Catalyst}]$
2	$\frac{\mathrm{d}[\text{Product P}]}{\mathrm{dt}} = \mathrm{K}_3 \times [\text{Intermediate I}] \times [\text{Reagent B}]$

An important aspect of employing a model for the selection of a design space is ensuring that the model is applicable at conditions and scales other than those employed for building the model. With this comparison, first we have the guarantee that the model can predict consistent results since the activation energies fits with the DFT calculations for a chemical mechanism that involves the same type of reactions, the difference is that they used a reagent different from reagent A. Thus, they observed much higher yields at $T_{ref.}$ [60-80]% then in our project [0-20]% at the same temperature, indicating that the activation energies of the mechanism using the other reagent is lower than when using reagent A.

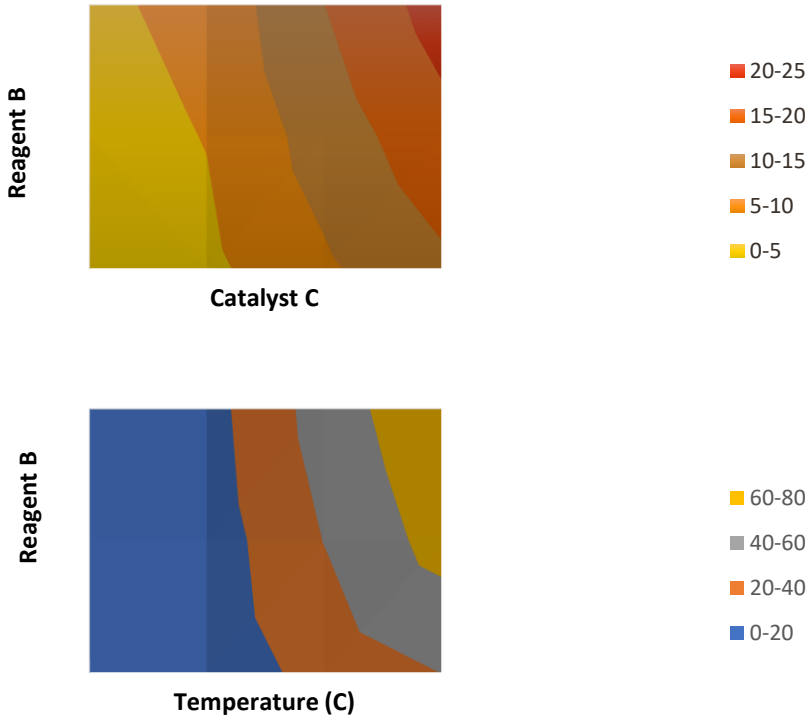

Figure 19 - Response contour plot of yield as a function of (above)number of equivalents of reagent B and number of equivalents of catalyst C, using solvent S at $T_{ref.}$ and (below) temperature and number of equivalents of reagent B, using a a value between [0-2] equivalents of catalyst C and solvent S

We conclude that the best conditions at $T_{ref.}$ and using solvent S, is using a number between [0-4] equivalents of catalyst C and [0-6] equivalents of reagent B in order to obtain 20-25% yields.

We defined as well that the best run to obtain maximum yields is using higher temperatures, (Tref+50)ºC, with a value between [0-6] equivalents of reagent B, and a value between [0-4] equivalents of catalyst C with solvent S. Concluding that the temperature is a critical process parameter.

3.2.5. EMPIRICAL MODELLING (DOE)

An empirical model was generated in parallel with the development of the mechanistic model for comparison of these approaches to model development.

We constructed a carefully selected set of experiments with the objective to identify which design variables affect the response – molar yield. For this, a screening design tool was made in which relevant factors were varied simultaneously called statistically experimental design or, design of experiments (DoE). We performed a set of experiments defining a standard reference

experiment (center point) and then perform representative experiments around it. The model was fitted using PLS (Partial Least Square) algorithm to establish a multivariate model between the factors and the response.

To define a design space, it was necessary to specify design ranges for all process parameters that would impact the reaction yield. Therefore, the process parameters were chosen according to prior knowledge work from a factor at a time approach. The reaction time was defined based on experience on the time needed for reaction to complete. A stability test was made to make sure if a reaction completes before ($time_{ref.}$ - 10) hours, the product would not decompose. Reducing, this way, the parameter space to five variables.

The resulting model was converted into a response contour plot that were used to determine where the best operating conditions are to be expected (the range of which factor).

Table 12 - The factors considered in DoE for batch reactions and its ranges

Factors	Range
Temperature (ºC)	(Tref to Tref+50)
Equivalents of catalyst	[0-4]
Equivalents of reagent B	[1-6]
Solvent composition %	[0-80]
Catalysts	Catalyst C, Catalyst A, Catalyst T

To capture the influence of each of three acids it was defined a qualitative factor in three levels (three acids).

We used a L18 (3 level) design construction of the experiences, resulting in 21 experiences (Annex B). The measured response was the molar yield after synthesis of ($time_{ref.}$ - 10) hours.

In Figure 20 we can observe the summary of fit of data. The leftmost bar represents R^2 it is called the *goodness of fit*, and is a measure of how well the regression model can be made to fit the raw data and it amounts to 0.977. R^2 varies between 0 and 1, where 1 indicates a perfect model and 0 no model at all. [29]

A much better indication of the usefulness of a regression model is given by the Q^2 parameter. Q^2 is the second bar from the left in and it equals 0.617. This parameter is called the goodness of prediction, and estimates the predictive power of the model. For a model to pass this diagnostic test, both R^2 and Q^2 should be high, and preferably not separated by more than 0.2 - 0.3. A substantially larger difference constitutes a warning of an inappropriate model. Generally,

a $Q^2 > 0.5$ should be regarded as good, and $Q^2 > 0.9$ as excellent, but these limits are application dependent.[29]

The third bar in the summary of fit plot is called model validity and it equals to 0.414. It reflects whether the model is appropriate in a general sense. The higher the numerical value the more valid the model is, and a value above 0.25 suggests a valid model.[29]

Finally, the rightmost bar in the summary of fit plot is called the reproducibility diagnostic tool and it amounts to 0.991. This performance indicator is a numerical summary of the variabilities plotted in the replicate plot.[29]

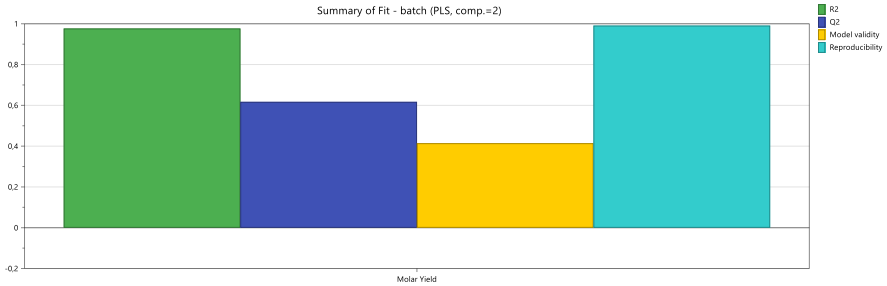

Figure 20 - Summary of fit plot for the regression model

After analyze the samples from the reactions, a simple exploratory data analysis by principal component analysis (PCA) was performed for outliers detection. The model presented two principal component analysis, the first one amounts a R^2 of 0.896 and a Q^2 of 0.735 and the second one a R^2 of 0.965 and a Q^2 of 0.827. The score plot is shown in Figure 53.

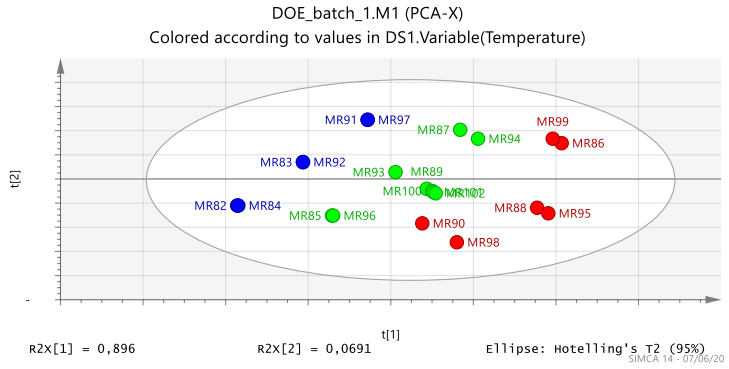

Figure 21 - Score plot for the first and second principal component of each reaction. The blue ones were performed at $T_{ref.}$, the green ones at ($T_{ref.}$+25), the red ones ($T_{ref.}$+50)ºC with ($T_{ref.}$+25)% confidence limit.

In Figure 22 we can observe that the variables that have more influence on the yield are temperature, water composition in the system, the use of catalyst C and the number of equivalents of reagent B. The equivalents used of catalyst, catalyst A has no impact on the system. Clearly, with the catalyst C we obtained the highest yields whereas with solvent T we obtain the lowest yields. The average yields across the nine experiments using catalyst C as the catalyst is between [20-40]%. The corresponding number for catalyst T is [0-20]%.

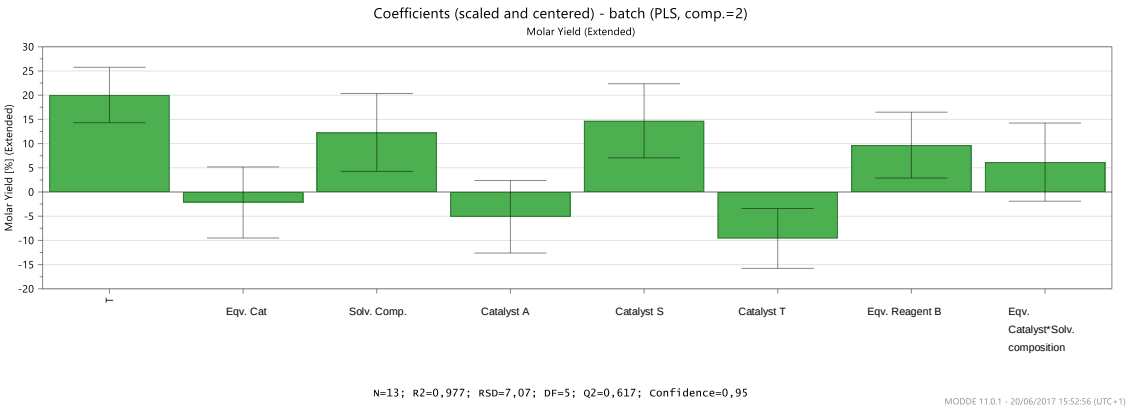

Figure 22 - Regression coefficient plot of batch regression model

One way of exploring the cross-terms consists of creating interaction plots. In Figure 23 with the respect of the interaction between the acids (catalyst A, catalyst C and solvent T) with the temperature. Better are the yields when the temperature is higher using catalyst C.

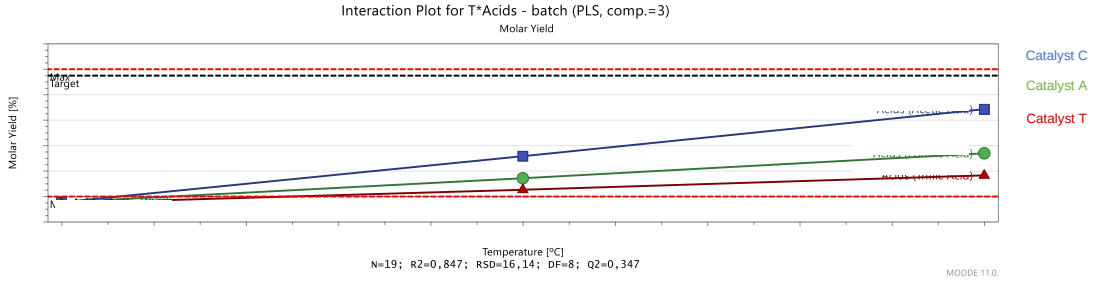

Figure 23 - Interaction plot for two cross terms: the effect of temperature using the three acids in the yield.

In Figure 24 we can see the interaction between the temperature and the nº of equivalents of reagent B used and we can conclude that the yield improves not only with higher temperatures but with more reagent B in the solution.

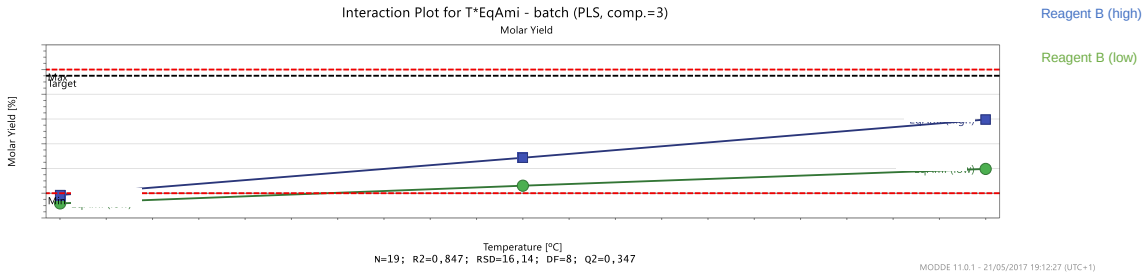

Figure 24 - Interaction plot for two cross terms: The effect of temperature vs. nº of equivalents of reagent B in the yield.

Figure 25 shows that we should position new (verifying) experiments in the down-right corner, obtaining the best yields using catalyst C.

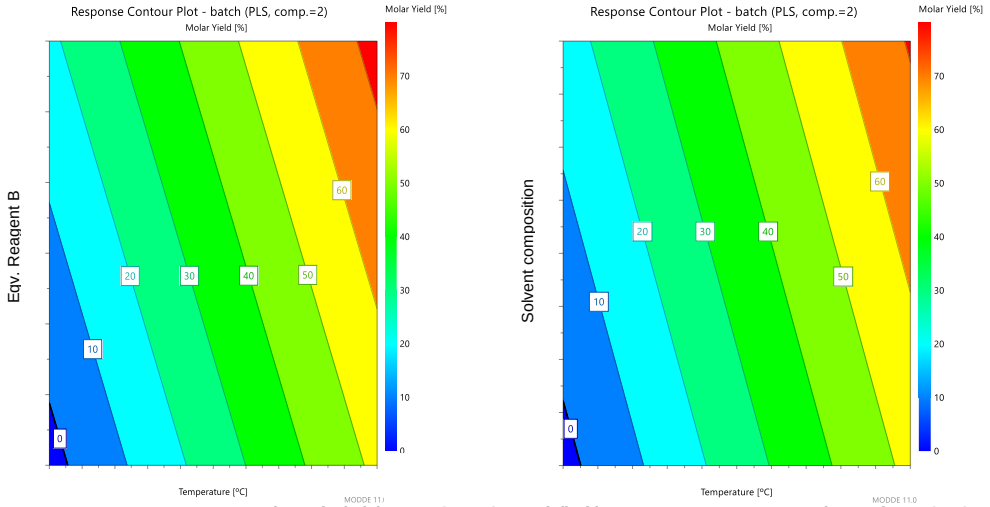

Figure 25 - Response contour plot of yield as a function of (left) temperature vs number of equivalents of reagent B, with 2 equivalent of catalyst C and solvent S; (right) temperature vs solvent composition, with a value between [0-6] equivalents of reagent B and a value between [0-4] equivalents of catalyst C.

OPTIMIZATION

MODDE® has an application called "*optimizer*" that calculates, with an interval of confidence of ($T_{ref.}$+25)%, the best condition to perform experiences for each catalyst based on the best yield. Moreover, this application determines which factors have more influence on the yield as we can see below for catalyst C:

Response	Criterion	Value
Molar Yield	Maximize	**[60-80]**

Table 13 - Optimized conditions estimated using DoE

Factor	Role	Value	Factor contribution
Temperature (ºC)	Free	$T_{ref.}$ + 50	57.64
Equivalents of Acid	Free	[0-4]	8.27
Solvent composition. % (v/v)	Free	[0-80]	11.93
Acid	Constant	Catalyst C	-
Equivalents of Reagent B	Free	[1-6]	22.16

3.2. CONCLUSION

The first approach of this thesis was to understand the reactional system to produce *product P* using reagent A and reagent B and determine which are the best process conditions. Firstly, we built the experiences using one factor at a time approach where we obtained low yields between [0-40]%. Thus, we decided to perform a screening, using design of experiments in order to understand the range of parameters that we should work to obtain higher yields. We performed 21 reactions obtaining maximum yields of [60-80]%. With the DoE approach, we can conclude that a carefully selected *set* of experiments, based on statistical experimental design can save time and costs. To reach [20-40]% yields, using a factor at a time approach, we took several weeks while using a DoE approach, we took 2 weeks to reach a yields between [60-80]%, which means increasing yields in [20-40]% from what we already knew. Moreover, we could determine which are the most influential factors: temperature and increase of reagent B loading, and the negligible ones: nº of equivalents of catalyst C and solvent S composition. Although based in prior knowledge (one factor at a time approach), it is known that with the increase of catalyst C, the yield increases so it would be interesting to perform a set of experiments with less factors to confirm this. We used three different catalysts: catalyst T, catalyst C and catalyst A and we concluded that catalyst C is better as shown in

Figure 23. In other words, DoE provided a reliable basis for decision-making, thus providing a framework for changing all the important factors systematically.

Additionally, we built a Dynochem® model, and values of kinetic constants (K_c), and energy of activation (E_a) were estimated for: (1) reagent A combines with the catalyst to form intermediate I, this way activating the C–O bond of reagent A and were found to be [1.00E-6 to 9.00E-2] L/mol.s and [30-200] kJ/mol respectively (2) a nucleophilic addition of reagent B to intermediate I forming the product P and were found to be [1.00E-6 to 9.00E-2] L/mol.s and [100-300] kJ/mol respectively Furthermore, the mechanistic model can explore transient conditions that would be inaccessible to an empirical model for which only the exact process used in the DoE experiments are accessible for predictions. In instances where a mechanistic model does not fit well due to a complex reaction system, an empirical model may be a desirable approach to obtain predictions for design space development.

Although we obtained reasonable yields [60-80]%, inevitably there are formation of side-products. We did not perform analysis in order to determine the structure of side-products, for example with advanced solid-state ^{13}C NMR. But we concluded that we can avoid the formation of those solids diluting the solution and performing reactions with less time, which means increasing temperature in order to increase the yield.

Finally we obtained the design space, determining which are the best conditions (in the range that we studied) to perform reactions in lab scale; using [0-80]% composition of solvent S, a value between [0-4] equivalents of catalyst C, a value between [0-6] equivalents of reagent B and (Tref+50)ºC.

Besides the reactions, we have defined a reproducible HPLC method, an appropriate work up and a full characterization of the product was done.

4. SYNTHESIS OF QUATERNARY AMMONIUM SALTS USING CONTINUOUS TECHNOLOGIES

4.1. INTRODUCTION

Synthetic chemists are under increasing pressure to discover and developing new scalable methodologies. Micro reaction technology is generally defined as the continuous flow processing of reactions within designed channels of 10-500 μm diameter and it attempts to develop reactional methods in the laboratory that are easily adapted to the production scale thus reducing the time needed between the passage between the two scales. [30,31]

4.1.1. FLOW CHEMISTRY

For liquid phase transformations at high temperature and pressure, capillary or tubular reactors of stainless steel are most often used. Tubular reactors derived from metals can withstand high temperatures and pressures generally required for most of organic syntheses.[31] Owing to its strength, durability, and corrosion resistance (except against very strong acids), stainless steel is the most widely used and easily available metallic alloy. The popularity of stainless steel can be attributed to the easy availability of coils and appropriate fittings which today are used routinely for analytical instrumentation such as HPLC and GC equipment.[32] In Table 14 we can see the application range of coil materials:

Table 14 – Application range of coil materials (Adapted from [32])

Application	PTFE	PFA	FEP	SST
Low T/P (<50ºC,<($P_{ref.}$ + 2) bar)	✓	✓	✓	✓
High T/P (<($T_{ref.}$ + 80)ºC,<20 bar)	⚠	⚠	⚠	✓
Very high T/P (>($T_{ref.}$ + 80)ºC,>20bar)	✗	✗	✗	✓
UV-Vis	⚠	⚠	✓	✗
Corrosive reagents	✓	✓	✓	⚠

✓ - ok to use; ⚠ some concerns, check database; ✗ not feasible

The use of back-pressure regulators in combination with standard HPLC pumps allows the processing of reaction mixtures at high pressures up to the maximum working limits of the reactor and of the other accessories used.[32] Back pressure regulators (BPR) are special valves which are installed to operate at a constant upstream system pressure. Working at elevated pressures not only allows processes to be performed above the boiling point of the reaction media but also enables superior control and rate enhancement when volatile or gaseous reagents or intermediates are employed. In Figure 26 we can see the general schematic diagram of a general flow set-up.[31]

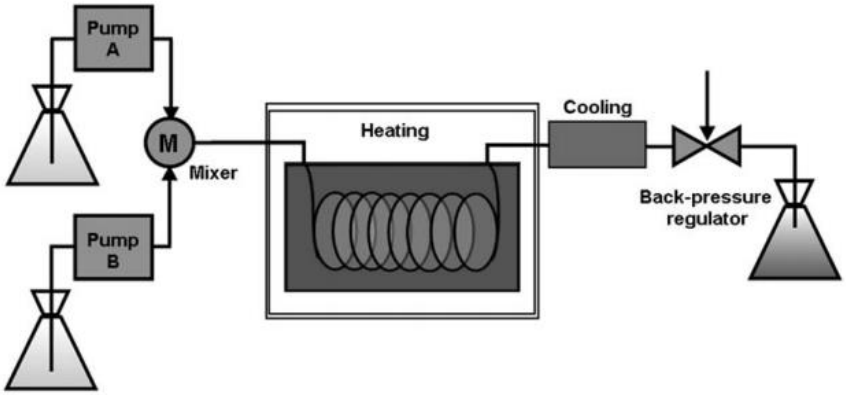

Figure 26 - General schematic diagram of a capillary/tubular reactor capable of performing organic synthesis under high temperature/pressure continuous flow conditions. Reproduced from [31]

Often mixing is highly influential in the conversion and selectivity of reactions.[33] Therefore, the degree to which mixing influences a reaction should be a major question when deciding whether to conduct an experiment in flow. Therefore, when deciding whether to conduct an experiment in flow, the mixing influence in the reaction should be taken into account. Mixing describes the way two phases come together and become intertwined. Batch and flow reactors exhibit different mixing pattern which in combination with reaction kinetics will determine if flow conditions are beneficial or not.[34] Additionally, the increased surface area to volume ratio of microreactors effectively increases mass transfer by 2 orders of magnitude, enhancing rates of reactions where mass transfer is rate limiting.[32]

Reactions where mixing is not highly influential can still benefit from continuous flow conditions. For example, flow conditions often outperform batch reactors for highly exothermic reactions that require cooling. Here, process intensification (high-temperature/high-pressure) can greatly reduce the reaction time. Finally, both heated and cooled reactions will be enhanced in flow when the product to side-product ratio is dictated by a small difference in transition state energies.

The influence of temperature in reactions is typically expressed using the Arrhenius rate law, derived from the observation that the reaction rate increases exponentially when the

temperature is increased. The expression below (3) illustrates a direct relationship between the absolute temperature and the rate constant of the reaction (K_c). Therefore, reactions which are prohibitively slow at room temperature can be sped up by heating.[32]

$$K_c = \mathrm{A} \times \mathrm{e}^{\frac{\mathrm{E_a}}{\mathrm{RT}}} \quad \textbf{(3)}$$

For a heated batch reaction, the reaction vessel is equipped with a stir bar and a condenser to prevent loss of solvent. It is necessary high boiling solvents when, under reflux conditions, we heat a reaction mixture to higher temperatures. To overcome this problems, it is used sealed vessels permits lower boiling point solvents for high-temperature reactions since solvents can be superheated above their boiling points.[33]

Finally, many different flow regimes can exist for liquid-liquid mixtures; however, laminar and slug flow are most commonly described for reactions in microchips and tube reactors. Common conditions in tube reactors (>0.25 mm) usually result in slug flow.[32] Slug flow is a liquid–gas two-phase flow in which the gas phase exists as large bubbles separated by liquid "slugs".[30] Generally, this happens when the pressure is not high enough.

4.1.2. BATCH VS. CONTINUOUS MANUFACTURING

In contrast to batch manufacturing, continuous manufacturing (CM) establishes a continuous flow of material exposed to a sequence of time-invariant unit operations, which can be monitored and controlled by in-line analysis tools to ensure that the final product complies with pre-defined quality attributes.[35] Furthermore, it contributes to the industry's response capacity by reducing the production time, reducing scale-up problems as development can be performed using the manufacturing equipment.[36] By eliminating scale-up, which may become a significant obstacle on the product's path to market, CM enables a more agile manufacturing process that can quickly be adapted to changes in the demand.

Different tools are required for API synthesis and for drug product manufacturing. During the API synthesis, continuous chemical reactors, which are well-established in other fields, can be used.[37] However, in the multi-step synthesis of APIs several problems need to be solved. Continuous crystallization is another critical step in the purification and final production of API crystals. Modelling of such systems has been reported in the literature.[35]

Batch processing has dominated the API industry due to available technologies. However continuous processing can often be more efficient and lucrative. Emerging technologies have opened up a lot of options in this area to make continuous more feasible in drug manufacturing.[38]

4.2. RESULTS AND DISCUSSION

4.2.1. DEFINING THE SET UP

All the components required for the set-up are represented in Figure 24, following standard HPLC devices.

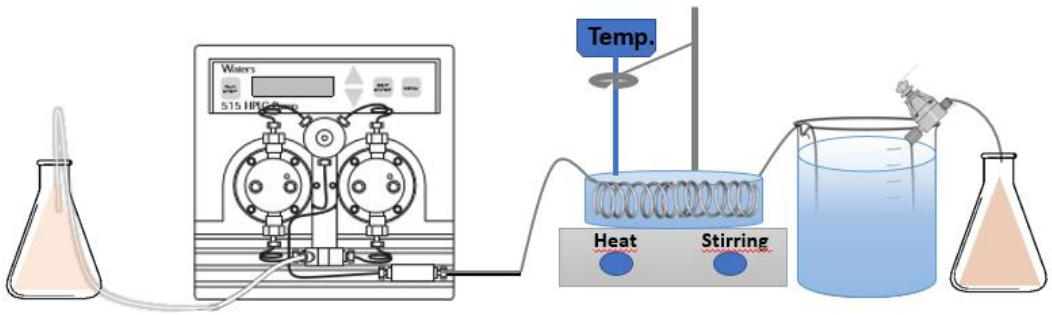

Figure 27 - Set up of the continuous system containing an HPLC pump (Waters 515), a coil of stainless steel with 1/16" of outside diameter, a heater plate, a temperature probe, a water at room temperature bath and a needle valve used as a back-pressure regulator

A BPR from Swagelok was used. Swagelok Integral Bonnet Needle Valve, 0.37 Cv, 1/4 in. MNPT, Regulating Stem;

Figure 28 – Needle Valve used as BPR in the set-up from Swagelok

The dimensions and composition of the tubing are crucial since it is in direct contact with the reagent stream. Physical parameters like the desired system pressure and chemical compatibility was considered. We used a connection of stainless steel from Swagelok.

Figure 29 – Connection of Stainless Steel OD: 1/16"

4.2.2. EFFECT OF THE CONCENTRATION

The first parameter that we studied in flow conditions was the concentration of the solution. We prepared samples in different concentrations with a value between [0-4] equivalents of catalyst C, a value between [0-6] equivalents of reagent B and solvent S, and residence time of ($Rt_{ref.}$ + 10) minutes to see if there is formation of by-products since we were experiencing new conditions (Table 15). While we were performing these study at 1 bar, we notice a liquid–gas two-phase flow, a phenomenon called slug flow. This happened because the pressure wasn't high enough for all reagents remain in liquid phase. Consequently, the compounds were retained in the coil, causing clogging. We increased the pressure for ($P_{ref.}$ - 1) bar slug flow was not observed but clogging was only not observed in a solution with concentration of 50mM.

Table 15 - Effect of the concentration in the flow system at ($T_{ref.}$ + 30)ºC, ($P_{ref.}$ - 1) bar

Concentration (mM)	Effect
1000	Clogging
500	Clogging
100	Clogging
50	No problems

4.2.3. EFFECT OF PRESSURE

In order to study the minimum pressure of work for all reagents remain in liquid phase we start performing reactions at ($P_{ref.}$ + 2) bar in the maximum temperature that the system could go, ($T_{ref.}$ + 105)ºC.

Table 16 - Effect of pressure in the flow system at ($T_{ref.}$ + 105)ºC

Pressure (bar)	Effect
5	Slug flow observation
10	Slug flow observation
13	Slug flow observation
16	No problems

Dynochem® offers an excel file that predicts the binary liquid liquid phase boundaries using NRTL (non-random two liquid) model. The non-random two-liquid (NRTL) model is utilized widely in phase equilibria calculations that are determined through regression of experimental data for a specific binary vapor–liquid equilibrium system.

The value of pressure observed experimentally at ($T_{ref.}$ + 105)ºC, ($P_{ref.}$ + 13) bar, fits with the value predicted by NRTL model.

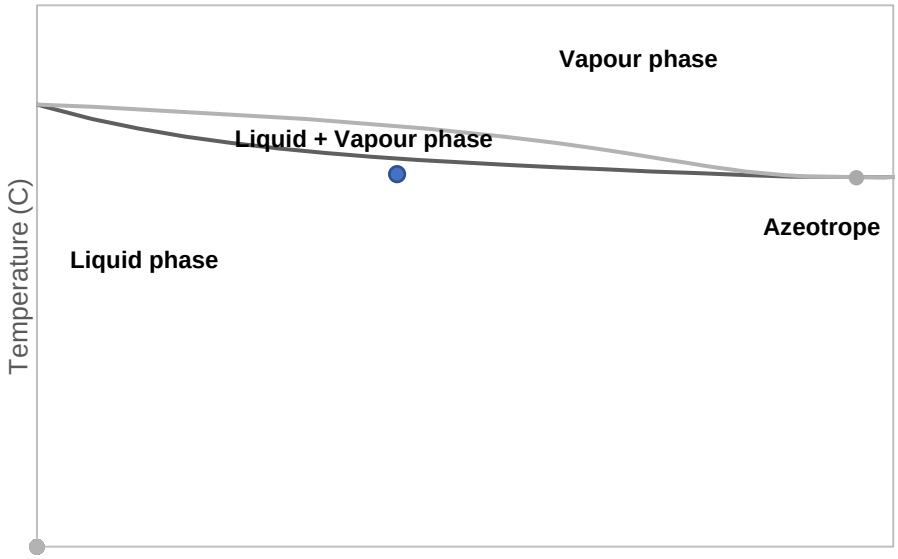

Figure 30 - Phase Diagram of solvent S, ($P_{ref.}$ + 13) bar predicted by NRTL model

Since in this thesis the solvent presents low boiling point, we inputted the conditions to use to predict the minimum pressure at different temperatures so when we perform reactions in different temperatures, we would know which pressure to use.

Table 17 - Determination of the minimum pressure necessary for all reagents remain in liquid state at high temperatures

Temperature (ºC)	Pressure (bar)
($T_{ref.}$ + 30)ºC	($P_{ref.}$ - 1)
($T_{ref.}$ + 55)ºC	($P_{ref.}$ + 2)
($T_{ref.}$ + 85)ºC	($P_{ref.}$ + 7)
($T_{ref.}$ + 105)ºC	($P_{ref.}$ + 13)

4.2.4. REACHING THE STEADY STATE

To determine the time to reach the steady state, we collected samples in a determined period of time. The steady state was reached at 3x the ($Rt_{ref.}$+10). (Figure 31)

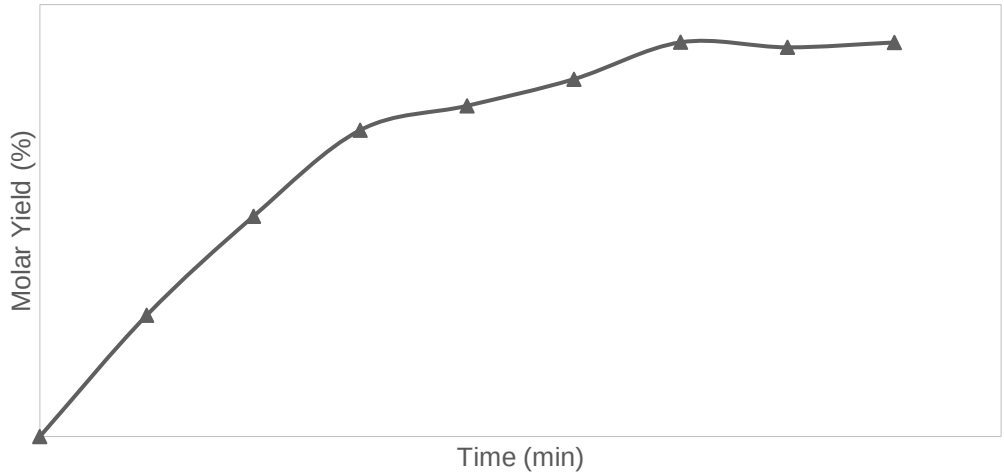

Figure 31 - Determination of the time needed for the reaction achieve the steady state (T: ($T_{ref.}$ + 105)ºC, P: ($P_{ref.}$ + 13) bar, Res. time: ($Rt_{ref.}$ + 10) min, C: 50 mM)

4.2.5. EFFECT OF TEMPERATURE

The effect of temperature on the reaction was studied by performing reactions at different temperatures while keeping other variables constant. It can be seen from Figure 32 that with an increase of temperature, the conversion of reagent A increases and the maximum yield is obtained at ($T_{ref.}$ + 105)ºC, between [80-100]%.

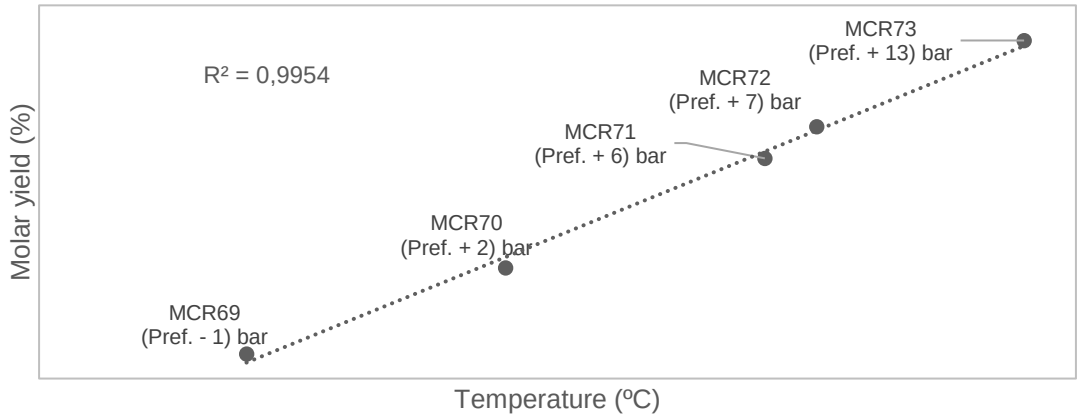

Figure 32 – Effect of temperature ($(T_{ref.} + 30)$, $(T_{ref.} + 50)$, $(T_{ref.} + 80)$, $(T_{ref.} + 85)$ and $(T_{ref.} + 105)$ºC) in the product yields in a reaction containing a solution of reagent A (50 mM), a value between [1-6] equivalents of reagent B, a value between [0-4] equivalents of catalyst C in solvent S, residence time of $(Rt_{ref.} + 10)$ minutes

We observed minimum by-products formation as shown in the chromatogram below (Figure 33), the solution had no solids in suspension.

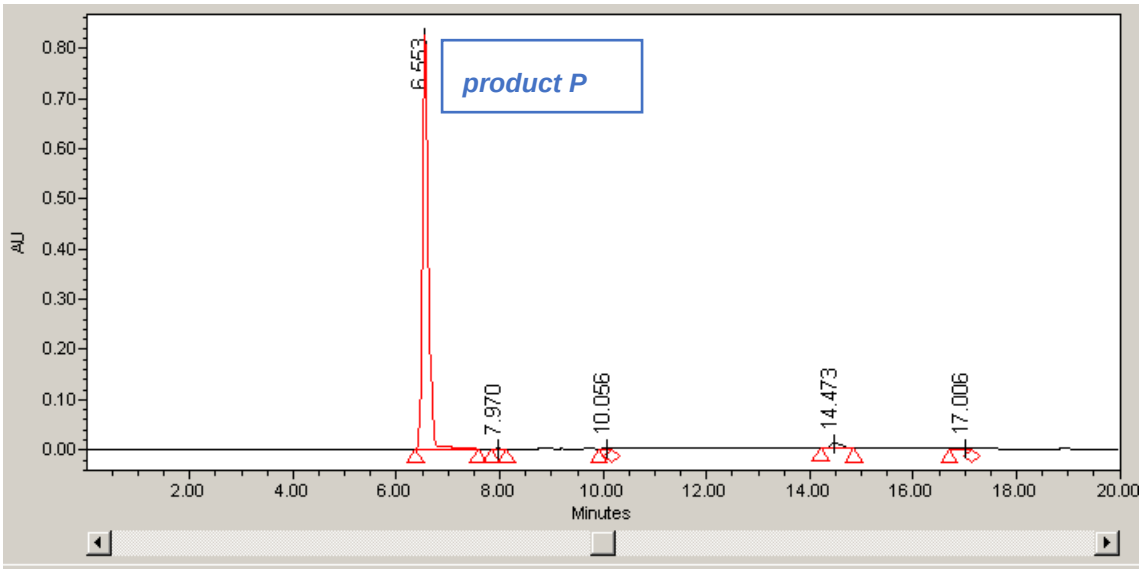

Name	Retention Time (min)	Purity1 Angle	Purity1 Threshold	PDA Match1 Spect. Name	PDA Match1 Angle	PDA Match1 Threshold	PDA Match1 Lib. Name	Area (µV*sec)	% Area	Height (µV)
	6.553							6736069	97.13	823618
	7.970							9161	0.13	1287
	10.056							19051	0.27	2902
	14.473							159920	2.31	10424
	17.006							11070	0.16	632

Figure 33 - Chromatogram of MCR73 without work up, area of product P peak presented % Area of 97.13%

We observed that by using flow conditions we could successfully avoid side reactions. We also confirmed that the yield improves with higher temperatures, as was already shown from batch studies.

After this, we performed a kinetic study with two different temperatures (($T_{ref.}$ + 85)ºC and ($T_{ref.}$ + 105)ºC) in the same conditions used above (Figure 32). One of parameter that we can better understand with the kinetic study is the effect of residence time. This study allows us to construct a mechanistic model of the reaction on Dynochem®.

4.2.6. MECHANISTIC MODELLING (KINETIC STUDY)

To construct the model on Dynochem® for flow conditions we had to:

1. Insert the reactions in the model, the same ones to construct the model in batch. (1) reagent A combines with the catalyst to form intermediate I, this way activating the C–O bond of reagent A (2) a nucleophilic addition of reagent B to intermediate I forming the product P.

2. Determine physical and chemical constants of the solution and its components, heat capacity, density, minimum pressure and vapour pressure;

Table 18 – Physical and chemical constants at ($T_{ref.}$ + 105)ºC

Heat Capacity – Cp (kJ/kg.K)	[3-5]
Density (kg/m^3)	[6-10]
Minimum pressure (bar)	[$P_{ref.}$+13]
Vapour pressure (bar)	[5-8]

3. Input those constants, the mechanism of the reaction and the conditions used (temperature, pressure, concentration, etc), including the characteristics of the set up.

Table 19 - Set-up work conditions

Length of the coil (m)	2.02
Volume of the coil (mL)	4
Feed rate (mL/min)	[0.1-8]

Mainstream Temperature (ºC)	22	
Bath Temperature (ºC)	($T_{ref.}$ + 85)ºC	($T_{ref.}$ + 105)ºC

We performed two reactions in different temperatures: ($T_{ref.}$ + 85)ºC and ($T_{ref.}$ + 105)ºC, in the same proportions of reagents and we collected samples at ($Rt_{ref.}$ – 9.5), ($Rt_{ref.}$ - 9), ($Rt_{ref.}$ - 8), ($Rt_{ref.}$ - 6), ($Rt_{ref.}$ - 2), ($Rt_{ref.}$ + 3.30) and ($Rt_{ref.}$ + 10) minutes for both reactions.

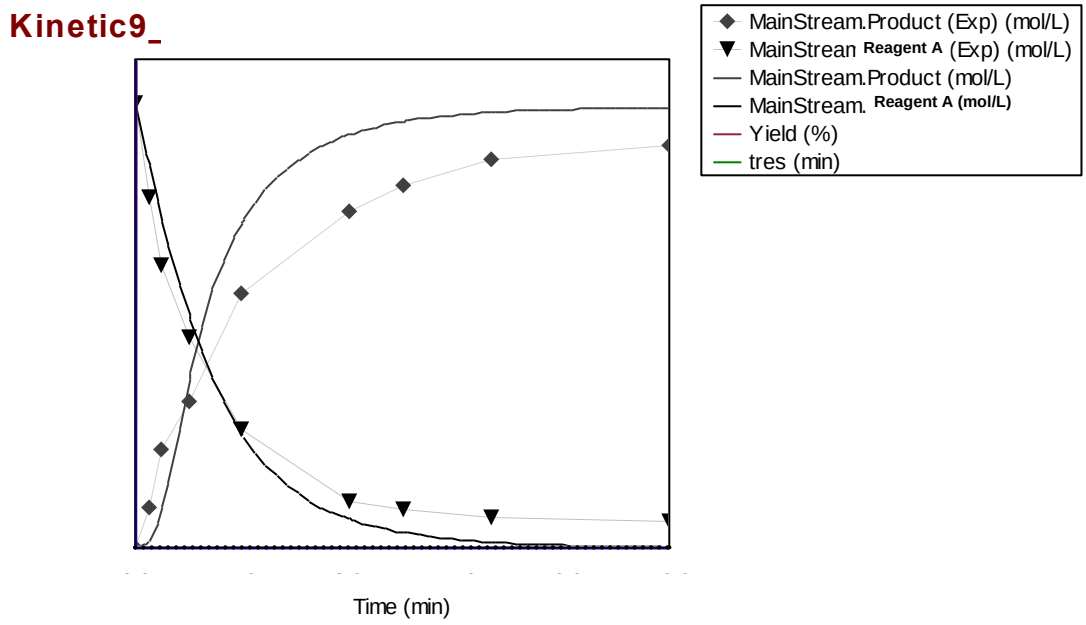

Figure 35 - Kinetic Study at ($T_{ref.}$ + 105)ºC (left) and ($T_{ref.}$ + 85)ºC (right). In a flask it was added reagent A, a value between [1-6] equivalents of reagent B, a value between [0-4] equivalents of catalyst C, solvent S. The solution was feed by an HPLC pump through the system.

As said in the section 4.2.5., Dynochem® gives us the sum of squares quadratic (SSQ) and this value can be interpreted as the sum of the errors between the predicted values and the observed ones of all points (in this case, we have 10). The lower is SSQ, the better is the fitting of the model.

Table 20 - Sum of squares quadratic expt 2: Kinetic ($T_{ref.}$ + 105)ºC

Scenario name	Data profile name	Number of Points	SSQ	Coef. of Determination
($T_{ref.}$ + 105)ºC	Solution.Reagent A	10.0	**0.0137**	0.9817
	Solution.Product P	10.0	**0.0358**	0.9826

In the table below (Table 21), we present the activation energy and kinetic constant determined by Dynochem®.

Table 21 - Activation energy (E_a) and Kinetic constant (K_c) for the four reactions inputted in the model and respective confidence interval

Reaction	Ea (kJ/mol)	K	Confidence interval
1	[40-200]	[1.00E-2 to 9.00E-1] L/mol.s	32.3%
2	[80-200]	[1.00E-2 to 9.00E-1] L/mol.s	18.5%

Obtaining this way, the rate expressions for each studied step:

Table 22 - Rate expressions

Reaction	Rate Expression
1	$\frac{\mathrm{d[Intermediate\ I]}}{\mathrm{dt}} = K_1 \times \mathrm{[Reagent\ A]} \times \mathrm{[Catalyst]}$
2	$\frac{\mathrm{d[Product\ P]}}{\mathrm{dt}} = K_2 \times \mathrm{[Intermediate\ I]} \times \mathrm{[Reagent\ B]}$

The DynoChem® design space exploration tool was used to simulate multiple scenarios.

From these two ($Rt_{ref.}$ + 10) minutes reactions, response surfaces were generated such as these in Figure 36. Each contour represents combinations of reaction temperature and residence time, at a specific composition of solvent.

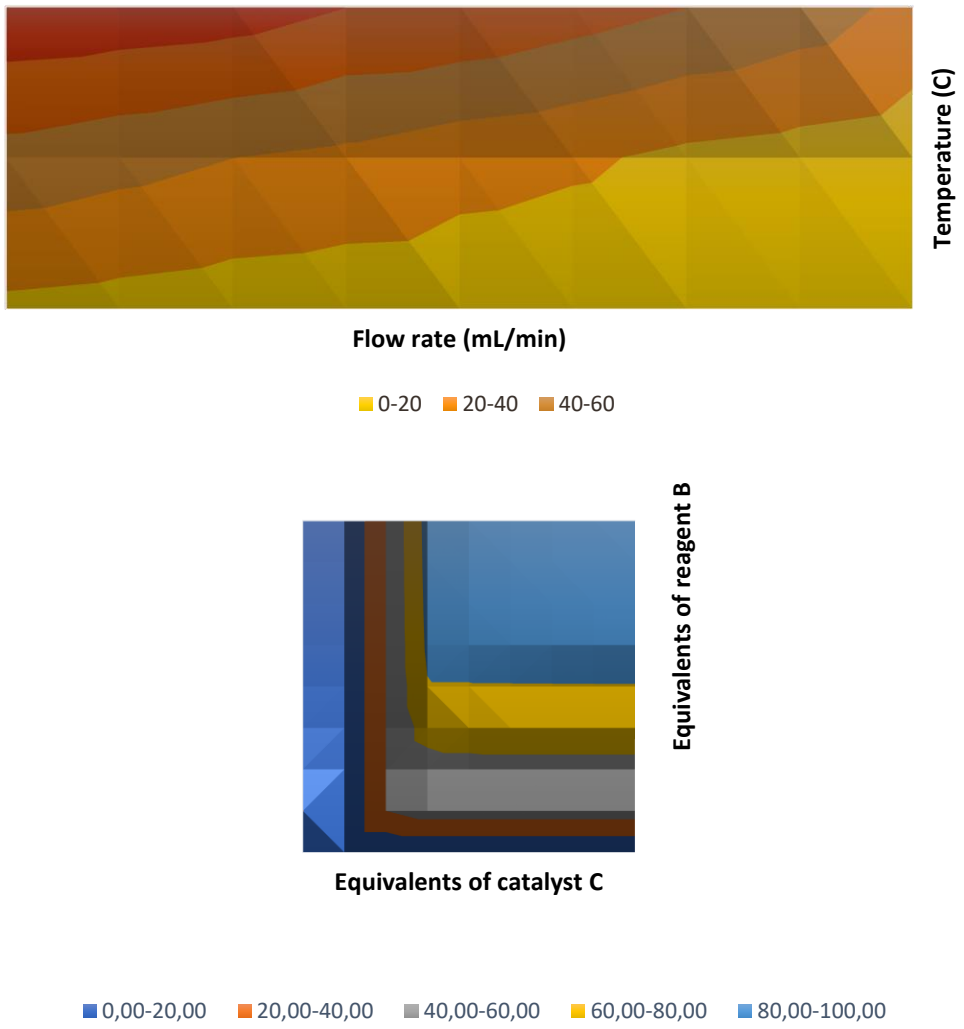

Figure 36 - Response contour plot of yield as a function of (above) temperature vs residence time, using a value between [0-4] equivalents of catalyst C, a value between [1-6] equivalents of reagent B and solvent S. (below) number of equivalents of reagent B vs number of equivalents of catalyst C, using solvent S at ($T_{ref.}$ + 85)ºC, with ($Rt_{ref.}$ + 10) minutes of residence time

4.2.7. EMPIRICAL MODELLING (DOE)

In order to check the influence of the parameters in the reaction since we now are using a different set-up from batch conditions, we decided to perform design of experiments. The solvent composition was removed from model development by selecting a value of solvent S. The elimination of this variable was justified based on experimental understanding of the impact of the solvent composition on the yield. We eliminated as well the screening of catalysts since we determined that catalyst C is the best one. Thus, the design space is limited to a fixed range of solvent compositions and catalyst C. However, this approach was adopted since it greatly simplified model development.

Table 23- Factors used to build the model on Modde®

Factors	Range
Temperature (ºC)	[$T_{ref.}$ + 30 to $T_{ref.}$ + 105]
Equivalents of catalyst	[0-4]
Equivalents of reagent B	[1-6]
Residence time	[$Rt_{ref.}$ – 5 to $Rt_{ref.}$ + 10]

After performing the reactions (Annex C), we obtained the summary of fit in Figure 37**, o**btaining an R2 of 0.725 and Q2 of 0.622. The validity of the model amounts 0.189 and the reproducibility was 0.929. The model was fitted using PLS algorithm, the same algorithm used to construct the model of batch reactions.

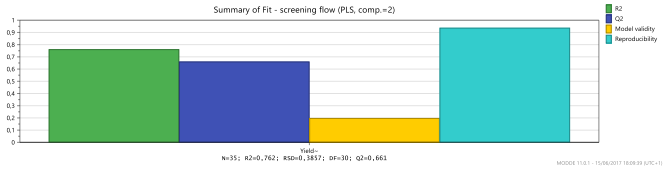

Figure 37 - Summary of fit for the regression model

After acquisition of samples from the reactions, a simple exploratory data analysis by principal component analysis (PCA) was performed to detect outliers before building the model. The model presented two principal component analysis, the first one amounts a R^2 of 0.968 and a Q^2 of 0.475 and the second one a R^2 of 0.998 and a Q^2 of 0.677. The score plot is shown in Figure 38.

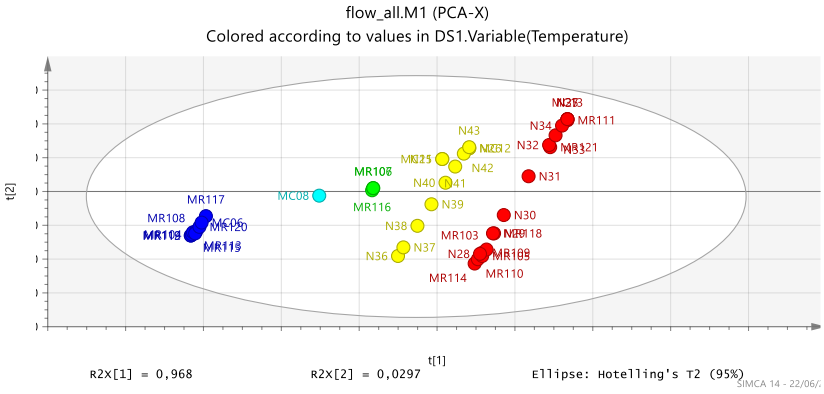

Figure 38 - Score plot for the first and second principal component of each reaction with ($T_{ref.}$+25)% confidence limit. The dark blue ones were performed at ($T_{ref.}$ + 30)ºC, the clear blue ones at ($T_{ref.}$ + 55)ºC, the red green ones at ($T_{ref.}$ + 67.5)ºC, the yellow ones at ($T_{ref.}$ + 85)ºC and the red ones at ($T_{ref.}$ + 105)ºC.

In Figure 39 we can see the histogram showing the distribution of the response (yield). In regression analysis, it is advantageous if the data of a response variable are normally distributed, or nearly so. This improves the efficiency of the data analysis, and enhances model validity. The histogram plot is useful for studying the distributional shape of a response variable.

To analyse the data we applied logarithmic transformation, obtaining a normal distribution of the yields.

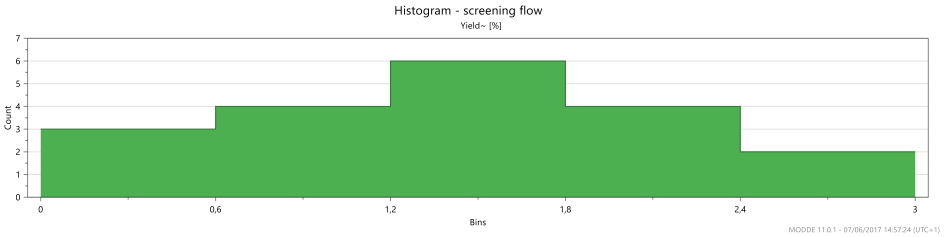

Figure 39 - Histogram of the data

After this pre-treatment of data we could build the model for flow conditions.

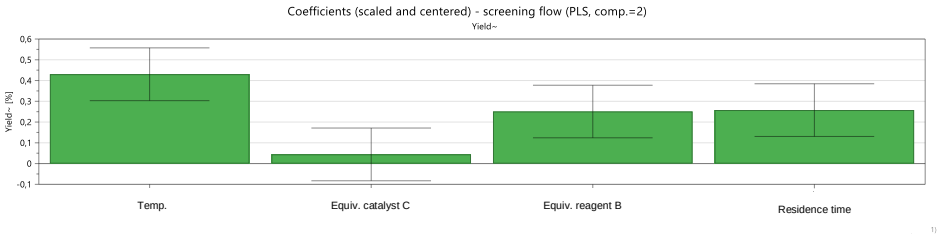

Figure 40 - Regression coefficient plot of flow regression model

With Figure 40 we can observe that the variables that have more influence on the yield are temperature, the number of equivalents of reagent B and the residence time.

Figure 41 shows that we should position new (verifying) experiments in the up-right hand corner, obtaining the best yields at ($T_{ref.}$ + 105)ºC and higher residence times.

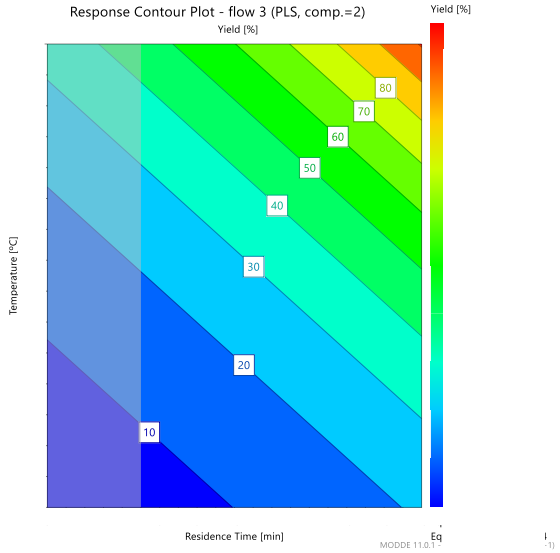

Figure 41 . Response contour plot of yield as a function of temperature and residence time

Figure 42 shows that we should position new experiments in the up-right hand corner, obtaining the best yields with higher number of equivalents of catalyst C and reagent B.

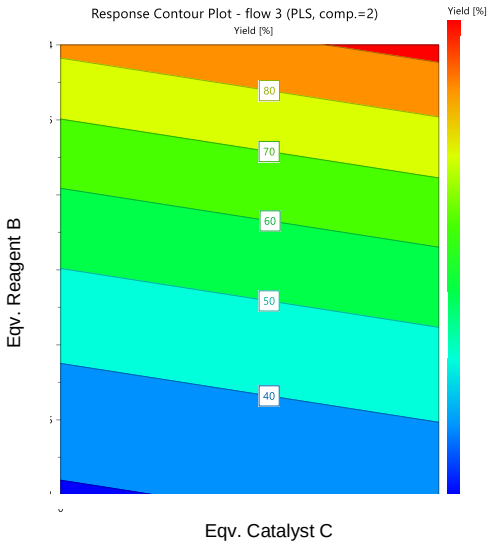

Figure 42 - Response contour plot of yield as a function of nº of equivalents of reagent B and nº of equivalents of catalyst C

Using MODDE® "*optimizer*" that calculates, with an interval of confidence of ($T_{ref.}$+25)%, the best condition to perform experiences based on the best yield.

Response	Criterion	Value
Molar Yield%	Maximize	**[80-100]**

Table 24 - Optimized conditions for the flow process estimated using DoE

Factor	Role	Value	Factor contribution
Temperature (ºC)	Free	$(T_{ref.} + 105)$ºC	43.04
Equivalents of Acid	Free	[0-2]	3.86
Equivalents of Reagent B	Free	[0-6]	29.52
Residence Time	Free	$[Rt_{ref.} – Rt_{ref.} + 10]$	23.57

4.2.8. COMPARISON BETWEEN THE MECHANISTIC AND THE EMPIRICAL MODELS – REGRESSION AND VALIDATION

Validation of the models was carried out with reactions with residence time of $Rt_{ref.}$ minutes, using a value between [1-6] equivalents of reagent B and a value between [0-4] equivalents of catalyst C at different temperatures.

Since we determined that the temperature is the factor that have more influence on the yield, we performed four reactions between $(T_{ref.} + 30)$ºC and $(T_{ref.} + 105)$ºC to validate the models therefore these four reactions were not used to construct them.

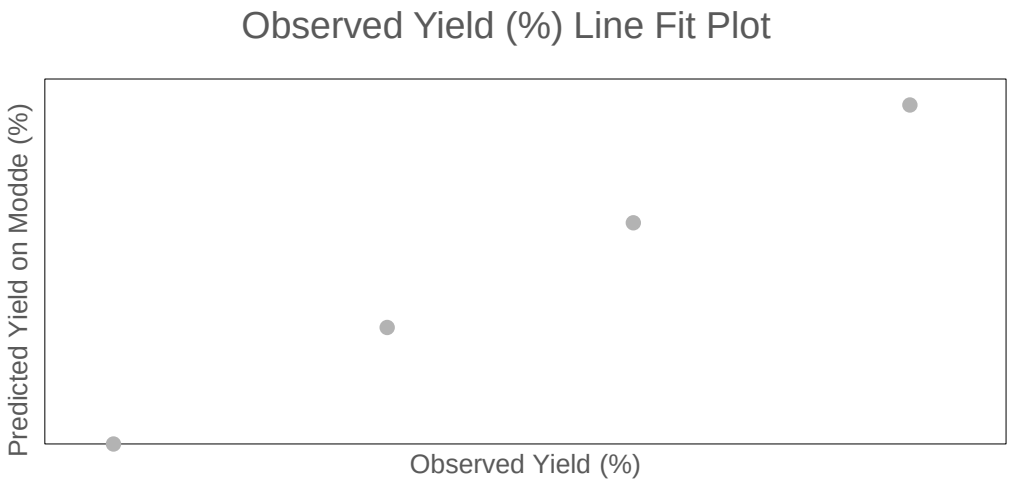

Figure 43 – The relationship between calculated with Modde® and observed response values of yields in the synthesis of product P

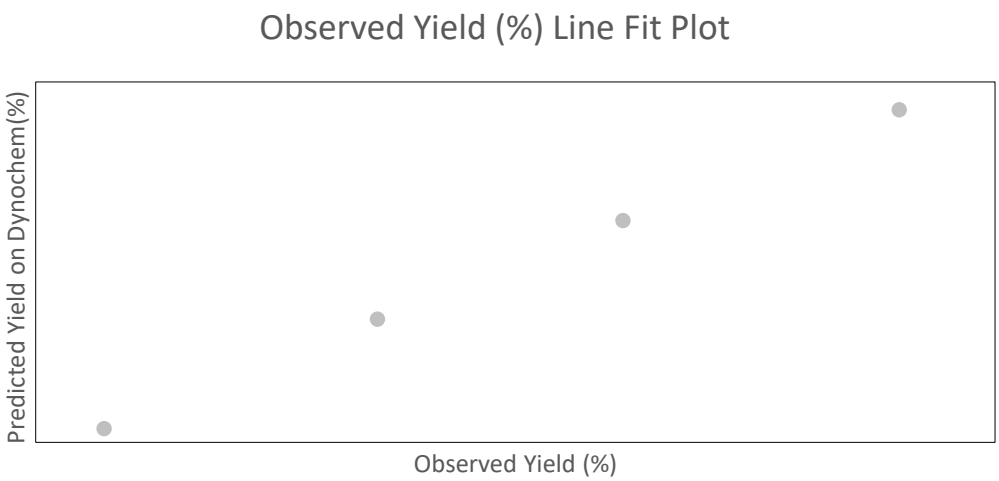

Figure 44 - The relationship between calculated with Dynochem® and observed response values of yields in the synthesis of product P

Table 25 - Comparing experimental data with the predicted data by Dynochem® and Modde®.

		Mechanistic Model		**Empirical Model**	
Temperature (ºC)	Experimental Yield (%)	Molar Yield (%)	RMSE	Molar Yield (%)	RMSE
($T_{ref.}$ + 30)ºC	[0-20]	[0-20]	2.05	[0-20]	1.17
($T_{ref.}$ + 55)ºC	[0-20]	[0-20]	4.60	[0-20]	7.61
($T_{ref.}$ + 80)ºC	[20-40]	[20-40]	2.99	[20-40]	8.38
($T_{ref.}$ + 105)ºC	[40-60]	[40-60]	4.60	[40-60]	5.62

About the mechanistic model, it was found that the experimental results match with the predicted ones, which indicates that the model fits well, with root mean square errors between 2-5%. Thus, it can be concluded that the Dynochem® model can be used for the estimation of kinetic and optimum process parameters, performing minimum experiments (in our case, just two reactions were performed).

About the empirical model, the predicted yields presented root mean square errors between 1 and 8%, which is reasonable. But considering the fact that to construct it we had to perform nineteen reactions against two reactions for mechanistic modelling, we can conclude that using DoE in flow chemistry is time consuming since we cannot do reactions in parallel as in batch case and in this project, the empirical model was not so accurate as the mechanistic one.

This case study outlined an example of an approach for defining a design space based on a mechanistic model. Although the predictions from an empirical model and a mechanistic model were found to be close to experimental data there are several advantages to utilizing a mechanistic model.

Another important advantage of a mechanistic model is the enhanced understanding of the mechanism and kinetics that is gained through developing it. Furthermore, the mechanistic model can explore conditions that would be inaccessible to an empirical model for which the reactions were performed in a limited range of the factors, and only inside of this range that we can predict the responses.

In our case, the process procedure benefited from the developed model and subsequent simulations. First, we performed reactions using a one factor at a time approach for three months, obtaining maximum yields between [20-40]%. When we performed the reactions after designing them in Modde®, we took two weeks to finish those, obtaining yields between [60-80]%. In the case of continuous manufacturing, we performed DoE to get information of the system and to make sure that there was no more interactions that the ones we already knew from batch manufacturing, since in flow, we have one more factor, which is the residence time and another ranges of temperature. We decided to perform DoE although before performing it, we already knew good conditions, had obtained yields between [80-100]%.

Lastly, In instances where a mechanistic model does not fit well due to a complex reaction system, an empirical model may be a desirable approach to obtain predictions for design space development.

4.2.9. ISSUES FOUND IN FLOW DEVELOPMENT

Slug Flow: Slug flow is a liquid–gas two-phase flow in which the gas phase exists as large bubbles separated by liquid "slugs". Generally, this happened when the pressure was not high enough, e.g.: when we were working at ($T_{ref.}$ + 105)ºC, the minimum pressure of work was ($P_{ref.}$ + 13) bar. If for some reason, the pressure decreased for ($P_{ref.}$ + 11) bar, slug flow was observed.

Pressure oscillations was observed when slug flow happened.

Clogging: Until we find a good concentration to work, we experienced clogging. of the flow unit, which happen at any place in the flow device. One of the main limitations for the continuous processing was clogging.

Run aways: Sometimes, when we experienced clogging, the pressure increases in seconds and the connections can not handle with those pressures, consequently the coils are separated.

Material incompatibilities: the needle valve clogging because the o-ring used inside the needle valve was made of Viton and this material is incompatible with some of the reagents. We had to buy o-rings of silicon which is a material compatible the reagents.

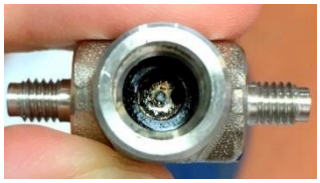

Figure 45 - Needle valve clogged because of o-ring material incompatibilities.

4.2.10. USE OF PROCESS ANALYTICAL TECHNOLOGIES (PAT)

To define an online control strategy we tried to make use of React-IR that is a real-time, *in situ* mid-infrared based system designed to study reaction progression and provide specific information about conversion of starting material, formation of intermediates and product which is very good for real-time process control.

We prepared solutions with different concentrations of the starting material:

Table 26 - Sensibility of the flow cell using React-IR

ConC. (M)	Reagent A	Reagent B	Catalyst C
0.1	No peaks observed	No peaks observed	No peaks observed
0.5	No peaks observed	No peaks observed	No peaks observed
2.6	Some peaks observed, low intensity	No peaks observed	No peaks observed
5.2	Observed, peaks well defined. Good resolution	Some peaks observed, low intensity	Some peaks observed, low intensity
7.8	Observed. Good resolution	Some peaks observed, low intensity	Some peaks observed, low intensity
10.4	Observed. Good resolution	Some peaks observed, low intensity	Some peaks observed, low intensity

Unfortunately, it was not possible to work with React IR since the minimum concentration to work with this equipment using those reagents (reagent A, reagent B and catalyst C) was 5.2M and the optimal concentration determined to the set-up used was 0.05M.

Even so, we tried to use a reactional mixture with 2.6M, with no success. Clogging was observed and the o-ring of the needle valve was deteriorated since it was made by Teflon (Viton), a material that is incompatible with some of the reagents.

4.3. CONCLUSION

In this thesis it was approached the development of a new process to produce quaternary ammonium salts from reagent A. Besides one factor at a time approach, we built an empirical and a mechanistic model for design space development that highlights a few key aspects that may apply in a future quality by design approach. We were successful in the development of the process using flow conditions, obtaining yields between [80-100]%, in a ($Rt_{ref.}$ + 10) minutes reaction, at ($T_{ref.}$ + 105)ºC, ($P_{ref.}$ + 13) bar, minimizing side reactions. These side reactions is a problem that chemical industry faces when using reagent A as starting material. We here in this thesis propose a process that makes use of reagent A as starting material and minimize the formation of side-products which hinder the purification and isolation of the main product.

The efforts to generate an empirical and a mechanistic model resulted in enhanced knowledge of the reaction, we were able to determine the best reactional conditions in order to increase the yield, to determine activation energies and kinetic constants of three steps of the main mechanism and of the side reaction that produces by-products.

Effects of various operating parameters on the synthesis of *product P* were identified using DoE statistics. It was found that the molar yield increases with an increase in reaction temperature, which is a critical process parameter and an increase of reagent B (a value between [0-6] equivalents) and catalyst C (a value between [0-4] equivalents) loading. The experimental data have been analysed using Dynochem® model, and values of kinetic constants (K_c), and energy of activation (E_a) were estimated for: (1) reagent A combines with the catalyst to form intermediate I, this way activating the C–O bond of reagent A, were found to be [1.00E-2 to 9.00E-1] L/mol.s and [40-200] kJ/mol respectively (2) a nucleophilic addition of reagent B to intermediate I forming the product P were found to be [1.00E-2 to 9.00E-1] L/mol.s and [80-200] kJ/mol respectively.

To validate the model, reactions in different conditions then the ones used to build both models (using Modde® and Dynochem®) were performed. It was found that the experimental results match with the predicted ones, which indicates that both model fits well although the model built with Dynochem® took two days in the laboratory and presented root mean square errors between 2 and 5% while the model built with Modde® took two weeks in the laboratory and presented root mean square errors between 1 and 8%. Thus, it can be concluded that the Dynochem® model can be used for the estimation of kinetic and optimum process parameters with performing minimum experiments.

Flow chemistry is advantageous for certain transformations; however, developing this flow process was time consuming. In one hand, for new transformations, which was our case, it was more convenient to screen concentrations, solvents, catalysts in batch because these variables could be tested simultaneously, whereas they would be done sequentially in flow. On the other hand, temperature and time optimizations were easier in flow because the coil

temperature could easily be changed and precise control of the reaction time was varied via flow rates.

Small-scale pressurized batch reactions are feasible, we used high-pressure vessels until certain temperature (for safety reasons, we didn't perform reactions above (Tref+50)ºC); however, higher scales could be dangerous or much more difficult to perform. It is known that flow chemistry with gas-liquid mixtures offers many benefits such as, improved interfacial mixing and safely achieving high pressures[32]. For these reasons, the reaction rate, scalability, and safety can be improved by using flow conditions.

The synthesis of *product P* from reagent A involves formation of solids during the reaction. This is a fact to consider when transposing reactions from batch to continuous, because precipitation in flow frequently results in the mixer, coil, or pressure regulator clogging and there is no universal solution to this problem. Although the reaction must be done in a lower concentration (50 mM) in flow than in batch (($T_{ref.}$ + 30)ºC mM) to avoid clogging and formation of by products, generally, in flow, faster mixing and better heat transfer will benefit the yield. Similarly, selectivity can be enhanced in flow as well. Since flow reactors generally have a narrower temperature profile than batch reactors, side reactions close in energy to the desired reaction can be reduced or eliminated. Additionally, for extremely slow reactions, intensification of reaction conditions may produce compounds in a timely fashion. While sealed vessels are a convenient small-scale option, preparative scale high-temperature, high-pressure reactions are much safer in flow.

An online control strategy was approached using React-IR® from Mettler Toledo but unfortunately the flow cell utilized had no sensibility for the range of concentrations used in the lab scale.

As technologies become more developed and commercialized, they may shift from high-cost/limited-benefit laboratory methods to tools for expediting research. While some of these processes are being developed mostly for industrial purposes, others aim to enhance discovery and synthesis for research laboratories. Currently, these methods are not practical for the average laboratory. Automated feedback optimization was chosen as an emerging reason to perform flow chemistry since recent progress in this field has shown promise for the everyday chemist. Currently, the equipment and process setup are too costly for the occasional user. Even so, this area is showing promise for the time of reaction optimization. The scientific method is a thought process for testing hypotheses and obtaining new knowledge.

5. CONCLUDING REMARKS AND FUTURE PERSPECTIVES

This thesis presents the development of a new process to produce new functionalized quaternary ammonium salts. We synthesized quaternary ammonium salts from reagent A using batch and continuous technologies that later will be utilized as an intermediate to produce an API. It presents an approach of employing a mechanistic and an empirical model that was effective in producing enhanced process knowledge and in defining a design space for it. Several aspects of this case study may be broadly applicable to process development within the QbD approach.

Continuous mode revealed to be more feasible to perform this reaction, not only because it was reached maximum molar yields between [80-100]% with the set up and conditions used, but also because is safer and allows a more precise control of the critical process parameters, for example, pressure was controlled by using a backpressure regulator. The ability to access another range of temperature and pressure, that in batch was not possible, expanded the screening range of the reactional parameters. Minimization of side-reactions also occurred possibly because of the enhance of mass transfer and efficient mixing in flow conditions.

The developed process using continuous mode, making use of an HPLC pump and a stainless steel coil, can be used to produce another quaternary ammonium salts with other functional groups and properties, embracing and covering applications that make use of reagent A to give quaternary ammonium salts.

The effort to perform the multiple reactions and assays engendered by a DoE and to build a model using a mechanistic approach is time-consuming but the quality and thoroughness of the information obtained outweigh the effort. The efforts resulted in enhanced knowledge of the process that not only guided the design space but also can be further utilized in finalizing the control process procedure (trying others PAT tools, per example) and performing a risk assessment.

Evaluating these parameters in light of business considerations, there were no readily apparent drivers to expand the design space to include higher reagent B equivalents (inefficient/costly use of raw materials), higher reaction temperatures, $>(T_{ref.} + 105)$ºC (increased energy consumption), or to increase the time – batch – or residence time – continuous – of the reaction (unnecessary increase of time). An additional business consideration is the incremental cost of model development in support of a dynamic design space strategy, which requires significant up-front resources for rigorous model characterization and quantification of model uncertainty and a long-term resource commitment for periodic model maintenance and revision.

6. GENERAL EXPERIMENTAL METHODS

Reagents

All chemicals, reagents and solvents for the synthesis of the compounds were of analytical grade, purchased from commercial sources, namely Sigma-Aldrich®, Merck, Acros and Alfa Aesar and these were used without further purification.

All material were washed in a dish machine and dried in an oven at ($T_{ref.}$+50)ºC.

Detection, isolation and purification of the reactional products

MS: Low resolution ESI mass spectra of the calcitocin experiments were carried on an ion trap mass analyser - *Thermo Scientific* LCQ Fleet Ion Trap LC/MS - equipped with an electrospray interface. Pro Mass for Xcalibur (Version 2.8) was used as the deconvolution software.

MIR: Spectroscopy *in situ* were performed using ReactIR 15 with liquid N_2 MCT Detector; using a probe interface: DS Micro Flow Cell 10µL (DiComp Diamond – tip); Resolution: Normal (8 wavenumbers); Spectral Range: 4000cm^{-1}-650cm^{-1};*Mettler Toledo*® equipped with iC IR™ (Version 4.3) software.

Characterization

NMR

^{1}H and ^{13}C NMR spectra were measured on an Ultrashield Bruker Avance II 300 spectrometer. Splitting patterns are indicated as s, singlet; d, doublet; t, triplet; q, quartet; m, multiplet; br, broad peak.

High Pressure Liquid Chromatography Analysis

The liquid chromatographic system is composed by a Waters® 2690 separation module with a Waters® diode array detector 906.

1st step of reaction column: Gemini, 3 µm C18 110 Å, LC Column 250 x 3 mm; Stationary Phase: C18 with TMS end capping; Solid Support: Fully Porous Organo-silica; Separation Mode: Reversed Phase; *Phenomenex;*

Method 1: The compounds were separated using gradient of from 5 to ($T_{ref.}$+25)% acetonitrile and water at a flow rate of 0.5 mL/min in a period of ($Rt_{ref.}$ + 10) min. The UV detection was at 250nm. 20 µL sample injection.

Synthesis of *product P* using batch

In a high pressure vessel (Ace Glass 8648-04 from Sigma Aldrich, LxOD: 10.2 cm x 25.4 mm) was added reagent A in solvent S, a value between [1-6] equivalents of reagent B and a value between [0-4] equivalents of catalyst C. The mixture was heated at $(T_{ref.} + 30)^0$C for $(time_{ref.} - 10)$ h. After the reaction finished, the solution was washed using an appropriate solvent (3x50mL) and the aqueous phase was evaporated at low pressure obtaining a brown oil, 30% yield calculated by HPLC.

Synthesis of *product P* using continuous manufacturing

A Waters® HPLC pump was used to feed the solution and the reactor was made from a Stainless Steel coil (outside diameter: 1/16 inches, inner diameter: 0.04 inches, $Volume_{total}$: 4mL, $length_{total}$:2.02m) immersed in a heated oil bath. (Flow: 0.4 mL/min, residence time: $(Rt_{ref.} + 10)$ min)

A needle valve (Swagelok Integral Bonnet Needle Valve, 0.37 Cv, 1/4 in. MNPT, Regulating Stem) was used as a back-pressure regulator was required to achieve the minimum pressure to maintain the solution in liquid state (according to the temperature used).

Another coil of stainless steel (outside diameter: 1/16 inches, inner diameter: 0.04 inches, lenght: 1.5 m) connected with the first one mentioned and before the needle valve, was immersed in a room temperature water bath to cool down the solution before the collection of the sample. This second coil was not considered to calculate the residence time.

The first coil was heated at $(T_{ref.} + 105)$ºC and the pressure was settled to $(P_{ref.} + 13)$ bar with solvent running through the coils. After achieving these conditions, a solution containing reagent A, a value between [1-6] equivalents of reagent B, a value between [0-4] equivalents of catalyst C, Solvent S was feed by an HPLC pump through the coils.

After the reaction finished, the solution was washed with an appropriate solvent (3x200mL) and the solvent was evaporated at low pressure obtaining a brown oil (Yield: between [80-100]% calculated by HPLC).

7.REFERENCES

1. US - Food and Drugs Administration. Guidance for Industry PAT — A Framework for Innovative Pharmaceutical. (2004).

2. Stegemann, S. The future of pharmaceutical manufacturing in the context of the scientific, social, technological and economical evolution. *Eur. J. Pharm. Sci.* **90,** 3612–3638 (2016).

3. US Department of Health and Human Services. *ICH Guideline Q8 - Pharmaceutical Development (R2)*. (Food and Drugs Administration; Center for Drug Evaluation and Research, 2009).

4. Snead, D. R. & Jamison, T. F. A Three-Minute Synthesis and Purification of Ibuprofen : Pushing the Limits of Continuous-Flow Processing. *Angew. Chemie - Int. Ed.* **54,** 983–987 (2015).

5. Mascia, S., Heider, P. & Zhang, H. End-to-End Continuous Manufacturing of Pharmaceuticals : Integrated Synthesis , Purification and Final Dosage Formation. *Angew. Chemie - Int. Ed.* **52,** 12359–12363 (2013).

6. Ghislieri, D., Gilmore, K. & Seeberger, P. H. Chemical Assembly Systems : Layered Control for Divergent , Continuous , Multistep Syntheses of Active Pharmaceutical Ingredients. *Angew. Chemie - Int. Ed.* **54,** 678–682 (2015).

7. US Department of Health and Human Services. *Q12: Technical and Regulatory Considerations for Pharmaceutical Product Lifecycle Management - Business Plan*. (Food and Drugs Administration; Center for Drug Evaluation and Research, 2014).

8. Plumb. k. Continuous Processing in the Pharmaceutical Industry. *Chem. Eng. Res. Des.* **83,** 730–738 (2005).

9. Nepveux, K., Sherlock, J. P., Futran, M., Thien, M. & Krumme, M. How development and manufacturing will need to be structured-heads of development/manufacturing May 20-21, 2014 continuous manufacturing symposium. *J. Pharm. Sci.* **104,** 850–864 (2015).

10. Hallow, D. M., Mudryk, B. M., Braem, A. D. & Tabora, J. E. An Example of Utilizing Mechanistic and Empirical Modeling in Quality by Design. *J. Pharm. Innov.* **5,** 193–203 (2010).

11. Weissman, S. A. & Anderson, N. G. Design of Experiments and Process Optimization. A Review of Recent Publications. *Org. Proc. Res. Dev.* **19,** 1605–1633 (2015).

12. Anderson, N. G., Burdick, D. C. & Reeve, M. M. Current Practices of Process Validation for Drug Substances and Intermediates Abstract : *Org. Proc. Res. Dev.* **15,** 162–172 (2011).

13. Looker, A. R., Ryan, M. P., Neubert-langille, B. J. & Naji, R. Risk Assessment of Potentially Genotoxic Impurities within the Framework of Quality by Design Abstract : *Org. Proc. Res.*

Dev. **14,** 1032–1036 (2010).

14. US Department of Health and Human Services. ICH Guideline Q11 - Development and manufacture of drug substances. (2012).

15. Lendrem, D. *et al.* DOE (Design of Experiments) in Development Chemistry : Potential Obstacles. *Org. Proc. Res. Dev.* **5,** 324 (2001).

16. Lehne, R. . & Rosenthal, L. *Pharmacology for Nursing Care*. (Elsevier, 2013).

17. Vardanyan, R. . & Hruby, V. *Synthesis of Essential Drugs*. (Elsevier, 2006).

18. Vogel, A., Furniss, B. S. & Hannaford, A. J. *Vogel's Text Book of Practical Organic Chemistry*. (Prentice hall, 1994).

19. Kapková, P., Alptüzün, V., Frey, P., Erciyas, E. & Holzgrabe, U. Search for dual function inhibitors for Alzheimer's disease: Synthesis and biological activity of acetylcholinesterase inhibitors of pyridinium-type and their Aβ fibril formation inhibition capacity. *Bioorganic Med. Chem.* **14,** 472–478 (2006).

20. Pernak, J. Synthesis of 3-substituted pyridinium salts. *Arkivoc* 889–904 (2000). doi:10.3998/ark.5550190.0001.606

21. Zhao T. & Sun G. Synthesis and Characterization of Antimicrobial Cationic Surfactants: Aminopyridinium Salts. *J. Surfactants Deterg.* **9,** 325–330 (2006).

22. Ilangovan, A., Venkatesan, P., Sundararaman, M. & Kumar, R. R. Synthesis, characterization and antimicrobial activity of 4-amino-1-alkyl pyridinium salts. *Med. Chem. Res.* **21,** 694–702 (2012).

23. Damiano, T., Morton, D. & Nelson, A. Photochemical transformations of pyridinium salts: mechanistic studies and applications in synthesis. *Org. Biomol. Chem.* **5,** 2735–2752 (2007).

24. Stark, A. & Seddon, K. R. *Encyclopedia of Chemical Technology*. (John Wiley & Sons, Inc., 2007).

25. Plechkova, N. V. & Seddon, K. R. *Methods and Reagents for Green Chemistry: An introduction*. (Wiley, 2007).

26. Maase, M. & Massonne, K. *Ionic Liquids IIIB: Fundamentals, Progress, Challenges, and Opportunities-Transformations and Processes*. (American Chemical Society, 2005).

27. Sowmiah, S. *Synthetic approach towards biomass derived pyridinium salts - phD Dissertation*. (2016).

28. Ingold, C. K. *Structure and Mechanism in Organic Chemistry*. (G. Bell & Sons, 1953).

29. Eriksson, L., Johansson, E., Kettaneh-Wold, N., Wikström, C. & Wold, S. *Design of Experiments: Principles and Application*. (Umetrics Academy, 2008).

30. Wiles, C. & Watts, P. *Micro Reaction Technology in Organic Synthesis*. (CRC Press,

2011).

31. Razzaq, T. & Kappe, C. O. Continuous Flow Organic Synthesis under High-Temperature / Pressure Conditions. *Chem. Asian J.* **5,** 1274–1289 (2010).

32. Plutschack, M. B., Us Pieber, B., Gilmore, K. & Seeberger, P. H. The Hitchhiker's Guide to Flow Chemistry. *Chem. Rev.* A-CT (2017).

33. Micro, C. & Bond, T. A. Developing Continuous-Flow Microreactors as Tools for Synthetic Chemists. *Synlett* **15,** 2382–2391 (2009).

34. Gervais, T. & Jensen, K. F. Mass transport and surface reactions in microfluidic systems. **61,** 1102–1121 (2006).

35. Rantanen, J. & Khinast, J. The Future of Pharmaceutical Manufacturing Sciences. *J. Pharm. Sci.* **104,** 3612–3638 (2015).

36. Wiles, C. & Watts, P. Continuous Flow Reactors , a Tool for the Modern Synthetic Chemist. *European J. Org. Chem.* 1655–1671 (2008).

37. Porta, R., Benaglia, M. & Puglisi, A. Flow Chemistry : Recent Developments in the Synthesis of Pharmaceutical Products. *Org. Proc. Res. Dev.* **20,** 2–25 (2016).

38. Allison, G. *et al.* Regulatory and quality considerations for continuous manufacturing May 20-21, 2014 continuous manufacturing symposium. *J. Pharm. Sci.* **104,** 803–812 (2015).

ANNEXES

Annex A

REACTIONS PERFORMED IN BATCH USING DESIGN OF EXPERIMENTS

Table 27 – Reactions performed in batch using design of experiments

Exp Name	Temp. (C)	Nº Eqv. Catalyst	Solvent comp. % (v/v)	Catalyst	Nº Eqv Reagent B	Molar Yield (%)
MCR82	$T_{ref.}$	[0-4]	[0-20]	Catalyst C	[1-3]	[0-20]
MCR83	$T_{ref.}$	[0-4]	[20-40]	Catalyst A	[1-3]	[0-20]
MCR84	$T_{ref.}$	[0-4]	[60-80]	Solvent T	[1-3]	[0-20]
MCR85	($T_{ref.}$+25)	[0-4]	[0-20]	Catalyst A	[1-3]	[0-20]
MCR86	($T_{ref.}$+25)	[0-4]	[20-40]	Solvent T	[1-3]	[0-20]
MCR87	($T_{ref.}$+25)	[0-4]	[60-80]	Catalyst C	[1-3]	[0-20]
MCR88	($T_{ref.}$+50)	[0-4]	[20-40]	Catalyst C	[1-3]	[40-60]
MCR89	($T_{ref.}$+50)	[0-4]	[60-80]	Catalyst A	[1-3]	[0-20]
MCR90	($T_{ref.}$+50)	[0-4]	[0-20]	Solvent T	[1-3]	[0-20]
MCR91	$T_{ref.}$	[0-4]	[60-80]	Solvent T	[3-6]	[0-20]
MCR92	$T_{ref.}$	[0-4]	[0-20]	Catalyst C	[3-6]	[0-20]
MCR93	$T_{ref.}$	[0-4]	[20-40]	Catalyst A	[3-6]	[0-20]
MCR94	($T_{ref.}$+25)	[0-4]	[20-40]	Solvent T	[3-6]	[0-20]
MCR95	($T_{ref.}$+25)	[0-4]	[60-80]	Catalyst C	[3-6]	[20-40]
MCR96	($T_{ref.}$+25)	[0-4]	[0-20]	Catalyst A	[3-6]	[0-20]
MCR97	($T_{ref.}$+50)	[0-4]	[60-80]	Catalyst A	[3-6]	[60-80]
MCR98	($T_{ref.}$+50)	[0-4]	[0-20]	Solvent T	[3-6]	[40-60]
MCR99	($T_{ref.}$+50)	[0-4]	[20-40]	Catalyst C	[3-6]	[60-80]
MCR100	($T_{ref.}$+25)	[0-4]	[20-40]	Catalyst C	[1-3]	[40-60]
MCR101	($T_{ref.}$+25)	[0-4]	[20-40]	Catalyst C	[1-3]	[40-60]
MCR102	($T_{ref.}$+25)	[0-4]	[20-40]	Catalyst C	[1-3]	[40-60]

Annex B

REACTIONS PERFORMED IN CONTINUOUS USING DESIGN OF EXPERIMENTS

Table 28 – Reactions performed in continuous using design of experiments

Exp Name	Temperature (ºC)	Equiv. of catalyst	Equiv. of Reagent B	Residence Time	Yield (%)
MCR112	($T_{ref.}$ + 30)	[0-4]	[1-3]	[$Rt_{ref.}$ -5]	[0-20]
MCR114	($T_{ref.}$ + 105)	[0-4]	[1-3]	[$Rt_{ref.}$ -5]	[0-20]
MCR119	($T_{ref.}$ + 30)	[0-4]	[1-3]	[$Rt_{ref.}$ -5]	[0-20]
MCR110	($T_{ref.}$ + 105)	[0-4]	[1-3]	[$Rt_{ref.}$ -5]	[0-20]
MCR104	($T_{ref.}$ + 30)	[0-4]	[3-6]	[$Rt_{ref.}$ -5]	[0-20]
MCR118	($T_{ref.}$ + 105)	[0-4]	[3-6]	[$Rt_{ref.}$ -5]	[20-40]
MCR108	($T_{ref.}$ + 30)	[0-4]	[3-6]	[$Rt_{ref.}$ -5]	[0-20]
MCR109	($T_{ref.}$ + 105)	[0-4]	[3-6]	[$Rt_{ref.}$ -5]	[0-20]
MCR113	($T_{ref.}$ + 30)	[0-4]	[1-3]	[$Rt_{ref.}$ +10]	[0-20]
MCR105	($T_{ref.}$ + 105)	[0-4]	[1-3]	[$Rt_{ref.}$ +10]	[0-20]
MCR115	($T_{ref.}$ + 30)	[0-4]	[1-3]	[$Rt_{ref.}$ +10]	[0-20]
MCR103	($T_{ref.}$ + 105)	[0-4]	[1-3]	[$Rt_{ref.}$ +10]	[0-20]
MCR120	($T_{ref.}$ + 30)	[0-4]	[3-6]	[$Rt_{ref.}$ +10]	[0-20]
MCR121	($T_{ref.}$ + 105)	[0-4]	[3-6]	[$Rt_{ref.}$ +10]	[60-80]
MCR117	($T_{ref.}$ + 30)	[0-4]	[3-6]	[$Rt_{ref.}$ +10]	[0-20]
MCR111	($T_{ref.}$ + 105)	[0-4]	[3-6]	[$Rt_{ref.}$ +10]	[80-100]
MCR116	($T_{ref.}$+67.5)	[0-4]	[1-3]	[$Rt_{ref.}$ +7.5]	[20-40]
MCR106	($T_{ref.}$+67.5)	[0-4]	[1-3]	[$Rt_{ref.}$ +7.5]	[20-40]
MCR107	($T_{ref.}$+67.5)	[0-4]	[1-3]	[$Rt_{ref.}$ +7.5]	[20-40]
N27 (MCR65)	($T_{ref.}$ + 105)	[0-4]	[3-6]	[$Rt_{ref.}$ +7.5]	[80-100]
N28 (MCR66)	($T_{ref.}$ + 105)	[0-4]	[3-6]	[$Rt_{ref.}$ - 9.5]	[20-40]
N29 (MCR67)	($T_{ref.}$ + 105)	[0-4]	[3-6]	[$Rt_{ref.}$ - 9]	[20-40]

N30 (MCR68)	($T_{ref.}$ + 105)	[0-4]	[3-6]	[$Rt_{ref.}$ - 8]	[20-40]
N31 (MCR69)	($T_{ref.}$ + 105)	[0-4]	[3-6]	[$Rt_{ref.}$ - 6]	[40-60]
N32 ($MCRT_{ref.}$)	($T_{ref.}$ + 105)	[0-4]	[3-6]	[$Rt_{ref.}$ - 2]	[60-80]
N33 (MCR71)	($T_{ref.}$ + 105)	[0-4]	[3-6]	$Rt_{ref.}$	[80-100]
N34 (MCR72)	($T_{ref.}$ + 105)	[0-4]	[3-6]	[$Rt_{ref.}$ + 3.3]	[80-100]
N35 (MCR73)	($T_{ref.}$ + 105)	[0-4]	[3-6]	[$Rt_{ref.}$ +10]	[80-100]
N36 (MCR74)	($T_{ref.}$+85)	[0-4]	[3-6]	[$Rt_{ref.}$ - 9.5]	[0-20]
N37 (MCR75)	($T_{ref.}$+85)	[0-4]	[3-6]	[$Rt_{ref.}$ - 9]	[0-20]
N38 (MCR76)	($T_{ref.}$+85)	[0-4]	[3-6]	[$Rt_{ref.}$ - 8]	[20-40]
N39 (MCR77)	($T_{ref.}$+85)	[0-4]	[3-6]	[$Rt_{ref.}$ - 6]	[20-40]
N40 (MCR78)	($T_{ref.}$+85)	[0-4]	[3-6]	[$Rt_{ref.}$ - 2]	[40-60]
N41 (MCR79)	($T_{ref.}$+85)	[0-4]	[3-6]	$Rt_{ref.}$	[40-60]
N42 (MCR80)	($T_{ref.}$+85)	[0-4]	[3-6]	[$Rt_{ref.}$ + 3.3]	[60-80]
N43 (MCR81)	($T_{ref.}$+85)	[0-4]	[3-6]	[$Rt_{ref.}$ +10]	[60-80]